TALLINN UNIVERSITY OF TECHNOLOGY
SCHOOL OF ENGINEERING
Department of Electrical Power Engineering and Mechatronics

ENERGIASALVESTITE JUHTIMISSTRATEEGIATE UURIMINE JA ARENDAMINE SAARTALITLUSES MIKROVÕRGULE

RESEARCH AND DEVELOPEMENT OF CONTROL STRATEGIES FOR ENERGY STORAGES IN AN ISLANDED MICROGRID

MASTER THESIS

Student: Nazli Cinay

Student code: 196637 AAAM

Supervisor: Tobias Häring

Co-supervisor: Prof. Dr.-Ing. Dr. h.c. Helmuth Biechl

Tallinn, 2020

AUTHOR'S DECLARATION

Hereby I declare that I have written this thesis independently.

No academic degree has been applied for based on this material.

All publications, major viewpoints and data of the other authors used in this thesis have been referenced.

".....” ..... 202…..

Author: .....

/signature/

Thesis is in accordance with terms and requirements

".....” ..... 202….

Supervisor: ….....

/signature/

".....” ..... 202….

Co-supervisor: ….....

/signature/

Accepted for defence

".....”.....202… .

Chairman of theses defence commission: .....

/name and signature/

ABSTRACT

Author: Nazli Cinay *Type of the work:* Master Thesis

Title: Research and development of control strategies for energy storages in an islanded microgrid

Date: January 2020 113 *pages*

University: Tallinn University of Technology

School: School of Engineering

Department: Department of Electrical Power Engineering and Mechatronics

Supervisor of the thesis: Tobias Häring

Co-supervisor: Prof. Dr.-Ing. Dr. h.c. Helmuth Biechl

Abstract:

The thesis consists of 113 pages, it contains 29 tables, 38 figures and 11 equations.

The goal of this thesis is to develop simplified mathematical models and control strategies for battery and flywheel storage systems to reduce high currents and charging cycles of the battery in an islanded microgrid.

In the first part of this thesis an overview of Lithium-ion batteries is given. A comparison with other competing storage systems (e. g. lead-acid, fuel cells etc.) is provided.

The second part of this thesis presents the development process of the battery and flywheel storage models. It gives an overview of the modelled microgrid with the battery and flywheel system, PV system and load profiles.

The third part describes the control strategies of the energy storage systems, whereas three tested scenarios and results are displayed in the fourth part of this work.

In the last part of the thesis, the financial aspect of the work was considered, and a conclusion is derived.

Keywords: battery energy storage, flywheel storage, SOC, PV, load profile, charging, discharging, microgrid, Matlab

LÕPUTÖÖ LÜHIKOKKUVÕTE

Autor: Nazli Cinay *Lõputöö liik:* Magistritöö

Töö pealkiri: ENERGIASALVESTITE JUHTIMISSTRATEEGIATE UURIMINE JA ARENDAMINE SAARTALITLUSES MIKROVÕRGULE

Kuupäev: Jaanuar 2020 113 *lk*

Ülikool: Tallinna Tehnikaülikool

Teaduskond: Inseneriteaduskond

Instituut: Elektroenergeetika ja mehhatroonika instituut

Töö juhendaja(d): Tobias Häring

Töö konsultant (konsultandid): Prof. Dr.-Ing. Dr. h.c. Helmuth Biechl

Sisu kirjeldus:

Lõputöö koosneb 113 lehest ning sisaldab 29 tabelit, 38 joonist ning 11 võrrandit.

Töö eesmärk on väljatöötada lihtsustatud matemaatilised mudelid ja juhtimisstrateegiad akule ja hoorattale. Et vähendada mikrovõrgu saartalitluses aku laadimis- ja tühjendamistsüklite arvu ning järske koormuste muutusi.

Magistritöö esimeses osas antakse ülevaade Liitium-Ion akudest, võrreldes neid teiste salvestuslahendustega nagu pliiakud, vesinikenergiasalvestitega

Töö teises osas on kirjeldatud akupatarei ja hooratas-energiasalvesti mudelite arendust. Samuti antakse ülevaade mikrovõrgu mudelist ja selle kõikidest komponentidest nagu akupatarei, hooratas, fotoelektrilised päikesepaneelid ja koormused.

Töö kolmandas ja neljandas osas kirjeldatakse kolme väljatöötatud energiasalvestite juhtimisstrateegiat ja katseid.

Töö viimane osa koosneb finantsanalüüsi osast koos tasuvuse hindamisega ning kokkuvõttest

Märksõnad: akupatare, hooratas-energiasalvesti, laetustase, fotoelektrilised päikesepaneelid, koormusmuster, laadimine, tühjendamine, mikrovõrk, Matlab.

THESIS TASK

Thesis title:	**Research and development of control strategies for energy storages in an islanded microgrid**
Student:	**Nazli Cinay, 196637AAAM**
Programme:	**Energy conversion and control systems**
Type of the work:	**Master Thesis**
Supervisor of the thesis:	**Tobias Häring, Prof. Dr.-Ing. Dr. h.c. Helmuth Biechl**
Validity period of the thesis task:	**09.02.2019**
Submission deadline of the thesis:	**03.01.2020**

_____	_____	_____
Student (signature)	Supervisor (signature)	Head of programme (signature)

1. Reasons for choosing the topic

Renewable energy sources in connection with energy storages are becoming more and more important. Shortage of available energy can be caused by scarcity of production capacities, raw material stocks, energy conversion infrastructure and by real shortage of power distribution capacities. As a result, microgrids can operate in islanded mode, which can be a solution in the area of meeting the short-term fluctuating energy demand requirements and the supply of energy during transitory power disturbances. This thesis will contribute to the existing work in the field by investigating the use of battery and flywheel energy storage system and their management in an islanded microgrid.

2. Thesis objective

The aim of this thesis is to develop control strategies for energy storages in an islanded microgrid. In purpose to increase the off-grid time of the system, reduce charging cycles for the battery storage for increased battery lifetime. Therefore, simplified mathematical models of battery and flywheel storage system are used.

3. List of sub-questions:

Is adding a flywheel storage financially reasonable?

Can the charging cycles and high currents of the battery storage be reduced by using a flywheel storage system?

Can the battery life be increased by integration of a flywheel storage system?

Which control strategy for flywheel and battery storage can increase the off-grid time the most?

4. Basic data:

Measurement data of existing PV station in Laastu Talu OÜ, Nõrava in Estonia, from Toomas Vinnal and Hardi Puusepp.

Certain load profile data from load profile generator.

Datasheets from manufacturers.

Results and data from previous Master Thesis.

5. Research methods

The research in this work is based on the analysis of literature and modelling of Matlab simulations. Matlab models are developed based on literature analysis and datasheets. The models of the microgrid components are then verified with simple test signals. Finally, scenarios are implemented to simulate the research objectives with the developed models. The data analysis is done in Matlab m.file.

6. Graphical material

Graphical materials include explanatory drawings, schematics, tables or diagrams, and Matlab simulation results, they are part of the main work.

7. Thesis structure

Introduction

1. State of the Art
    - 1.1. Microgrid
        - 1.1.1.Typical topologies
        - 1.1.2.On/Off grid operation
    - 1.2. Storage technologies
        - 1.2.1.General storage technologies
        - 1.2.2.Electrochemical storage systems
    - 1.3. Battery storage systems

1.3.1.Evaluation parameters

1.3.2.Reliability

1.3.3.Battery Management

1.4. Conclusion

2. Object modelling in Matlab

2.1. Battery model

2.1.1.Review of models in scientific papers

2.1.2.Description of the model

2.1.3.Verification of the model

2.2. Other microgrid components

2.2.1.Load profile

2.2.2.PV system

2.2.3.Flywheel model

2.3. Complete system

3. Control models and strategies of microgrid system

3.1. Description of battery control model

3.2. Description of flywheel control model

3.2.1.Moving average control

3.2.2.Custom control

4. Matlab simulation of control strategies and test scenarios

4.1. Scenario 1: PV with battery storage system

4.2. Scenario 2: PV with battery and flywheel MA control

4.3. Scenario 3: PV with battery and flywheel custom control

5. Financial analysis

6. Conclusion

8. References

Sources used in this work come from books, research articles, standards, ect. Some of the sources used are listed below.

A. Rahomoun, „Mathematical Modelling and Analysis of a Battery Energy Storage System for Microgrids,“ Ph.D. dissertation, School of Engineering, Tallinn University of Technology, Tallinn, 2017.

M T. Lawder, B. Suthar, P. W. C. Northrop, S. De, C. M. Hoff, O. Leitermann, M. L. Crow, S. Santhanagopalan, and V. R. Subramanian, „Battery Energy Storage System (BESS) and Battery

Management System (BMS) for Grid-Scale Applications," *Proceedings of the IEEE,* Bd. 102, Nr. 6, pp. 1014-1030, 2014.

I. D. Serna-Suárez, G. Ordóñez-Plata, G. Carrillo-Caicedo, "Microgrid's Energy Management Systems: A survey," in *2015 12th International Conference on the European Energy Market (EEM)*, Lisbon, 2015.

"Battery University," [Online]. Available: https://batteryuniversity.com/learn/article/how_to_prolong_lithium_based_batteries. [Accessed 16 November 2019].

9. Thesis consultants

Prof. Dr. Sc. Eng. Argo Rosin

10. Work stages and schedule

Literature research (29. March))

State of the art (24. May)

Introduction in Matlab Software (6. June)

Matlab object modelling (26. August)

Matlab control models (20. September)

Matlab simulation and scenarios (25. October)

Completing the final version of the thesis (28. November)

Table of contents

APPLICATION IN ENGLISH

03.01.2020

From: Nazli Cinay (196637AAAM)
To: Ivo Palu

Application

I, Nazli Cinay would like to request the permission to write this master in English due to the following reasons:

This thesis is prepared to obtain the dual master's degree from Kempten University of Applied Sciences and Tallinn University of Technology based on the international cooperation agreement between those two universities.

I, as an Erasmus student from Germany, am not sufficiently educated in Estonian to write a Master thesis in Estonian language.

Thank you for your understanding.

Nazli Cinay

Preface

The present master thesis was produced within the framework of my study abroad at the partner University, Tallinn University of Technology (TalTech) at the department of Electrical Power Engineering and Mechatronics.

The topic was developed together with my supervisor Mr. Tobias Häring and Prof. Dr. Sc. Eng. Argo Rosin at the Tallinn University of Technology. At this point I would like to thank Mr. Tobias Häring for supervising this master thesis and for his guidance and support. In addition, special thanks to Prof. Dr. Sc. Eng. Argo Rosin for the support before and during my time at TalTech.

I would also like to thank also my Prof. Dr.-Ing. Dr. h.c. Helmuth Biechl from my home university, University of Applied Sciences (UAS) Kempten, who introduced me the possibility to obtain the double master's degree from UAS Kempten and TalTech, based on the international cooperation agreement.

In addition, my thanks go to the entire department of Electrical Power Engineering and Mechatronics at TalTech and people I met in Estonia who helped me with their advice and made me feel welcome in Tallinn.

I also want to thank my family, who have always supported me on my way through my studies.

Tallinn, 03. January 2020

Nazli Cinay

List of abbreviations and symbols used

ACSW	Alternating Current Switch
BESS	Battery energy storage system
BMIS	Battery Mode Identification Systems
CLFC	Closed-Loop Feedback Controller
DER	Distributed energy resources
DES	Distributed energy storages
DG	Distributed generator
EDLC	Electrochemical double-layer capacitor
EMS	Energy Management System
ESS	Energy storage systems
MA	Moving average
PV	Photovoltaics
PVGIS	Photovoltaic Geographical Information System
RES	Renewable energy sources
Rpm	Rotation per minute
SOC	State-of-charge
SOCdiff	SOC difference
SOH	State-of-health
VRB	Vanadium-redox battery

List of tables

List of figures

Introduction

Energy is mandatory for the development of economy and Social life. It is also one of the major components of Society and is needed to create goods from natural resources [1]. The global economic development and energy standard improvement are complex processes and need the availability of an adequate and reliable supply of clean energy [2].

The awareness that clean energy is decisive for our Society to function on a daily basis originates from the energy crises in 1973 [2]. The term energy crisis was coined in the early 1970s and has become a synonym for a severe shortage of oil on world markets. Today's regional and continental energy crises can, in contrast to earlier crises, be caused by the shortage of available energy (caused by the scarcity of production capacities, energy conversion infrastructure or raw material stocks) or insufficient capacities for power transmission or distribution (e.g. power line capacities) [3].

The oil crisis of 1973 was a consequence of reduced oil production and the resulting artificially depressed supply of oil. It should therefore also be better described as an oil price crisis, because there was no substantial technical shortage of oil supply. The oil price crisis of 1979/1980 was caused by the war between Iraq and Iran, which led to a loss of supply and an uncertainty regarding the future supply of oil [3]. This was almost to be forgotten, if it were not for the rising awareness of other environmental problems such as acid rain, global warming and radioactive waste. These are still very much of importance today and each of these themes is related to our energy security. A lot of sectors are strongly depending on energy, e.g. work, environment, economics and international relations as well as our own personal livings, i.e. transportation, communication and housing [2].

The biggest historical challenge of the energy industry, its carbon dioxide emissions, which are unprecedented in recent geological history, is threatening the global climate. Stocks of fossil fuels such as oil, coal and gas are finite and increasingly difficult to produce, and more and more environmental damage is being established [4].

In this situation, the development of sustainable energy sources and their integration into the energy grids is essential. Renewable energy is derived from natural processes such as biomass, tidal power, hydropower, wind power, photovoltaics (PV) or geothermal power, that are renewed constantly and replacing conventional fuel in different areas like power generation, hot water /

space, transport fuels and rural (off-grid) energy services [5]. Thus, the benefits of renewable energies are obvious: they are practically inexhaustible, have less environmental impact and threats, no fuel costs and are available in a decentral manner. Their disadvantages include the low energy densities, which make high use of materials (investments) necessary. Even more problematic can be the fluctuating energy supply (e. g. the solar radiation intensity, wind speed), which makes backup power plants necessary [4].

As a result, the topic of energy storage technologies is becoming increasingly important. In this context the law of conservation of energy states that energy cannot be created or destroyed but can be transformed from one form to another. Thus, the total amount of energy in a system holds constant or is maintained: With an energy storage system a certain amount of energy can be stored at a certain time and then be discharged later when it is needed. Energy storages have a great importance in the area of meeting the short-term fluctuating energy demand requirements and the supply of energy during transitory power disturbances. They also reduce the need for emergency power generators and improve the operational performance of energy systems. This provides energy security with low environmental impact. Energy produced by renewable energy sources during off peak hours can be redistributed to on-peak times and balance fluctuating loads [6].

Energy storage is thought of as a technique for charging and discharging electricity. For example, a photovoltaic (PV) cell is a device that converts the sunlight, so called solar energy, into electricity. On this occasion the sunlight, which is hitting the solar thermal panels, is converting sunlight to heat, water or electricity etc. But these are not available at night and maybe unavailable due to weather conditions. Therefore, a storage or complementary power system is needed for off-grid applications to store energy during the day and to be able to make use of it at night. Off-grid applications are using either battery storage, which cause significant energy losses or engine generators, which is associated with high fuel costs [5].

This work will focus on the development of simplified mathematical models and control strategies for a battery management system in apartment buildings and on microgrid level. Based on PV systems as the only power source, maximum islanded mode operation time without a backup generator should be achieved. In aim to reduce the battery capacity for an ensured stable operation and the energy conversion losses of the battery system as well as to increase the battery lifetime. This has the additional benefit reducing the amount of raw material needed for battery production.

1 State of the Art

Power failures and long-term power failures due to natural disasters are occurring more frequently. The problem is, that many states rely exclusively on coal and gas-fired power plants for power generation and distribute electricity miles through often outdated infrastructure, which increases the error rate immensely. Therefore, the local power supply should be supported by so-called microgrids [7]. This chapter discusses the definition, basic topologies, concepts and components of microgrids. It will also show different storage technologies and typical parameters of battery storage systems.

1.1 Microgrid

Microgrid is defined as an integrated energy system consisting of interconnected loads and distributed energy storages (DES). It can operate connected to the grid or in an island mode [8]. A simplified representation of a microgrid is shown in Figure 1.1.

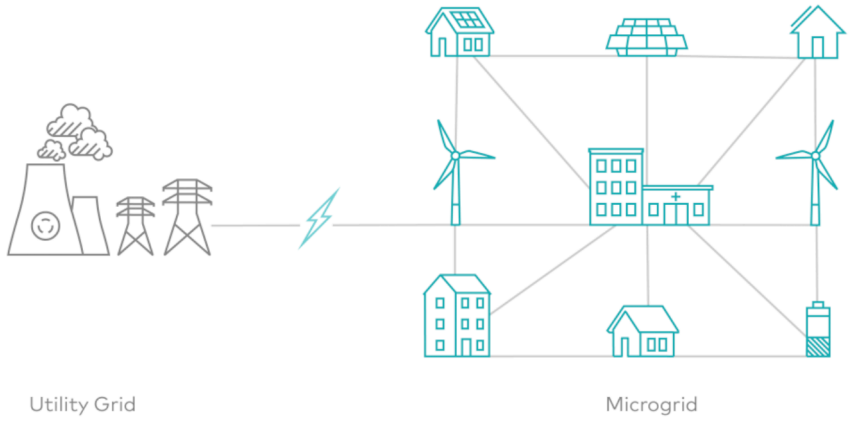

Figure 1.1 Simplified representation of a microgrid [7]

Microgrids powered by distributed energy resources (DER), for example wind, photovoltaic, biomass, micro turbine, fuel cell etc., are emerging and gaining increasing attention as effective means of integrating renewable distributed generators (DG) into existing power systems [9]. In future, high-level penetration of renewable energy resources in microgrids will pose a challenge for grid stability and supply reliability due to volatile power supply and instability issues. Therefore, distributed energy storages (DES), such as flywheel, battery, super capacitor or others, are playing

an important role in improving stability, strengthening reliability and ensuring security. Figure 1.2 shows a typical structure of a microgrid [9].

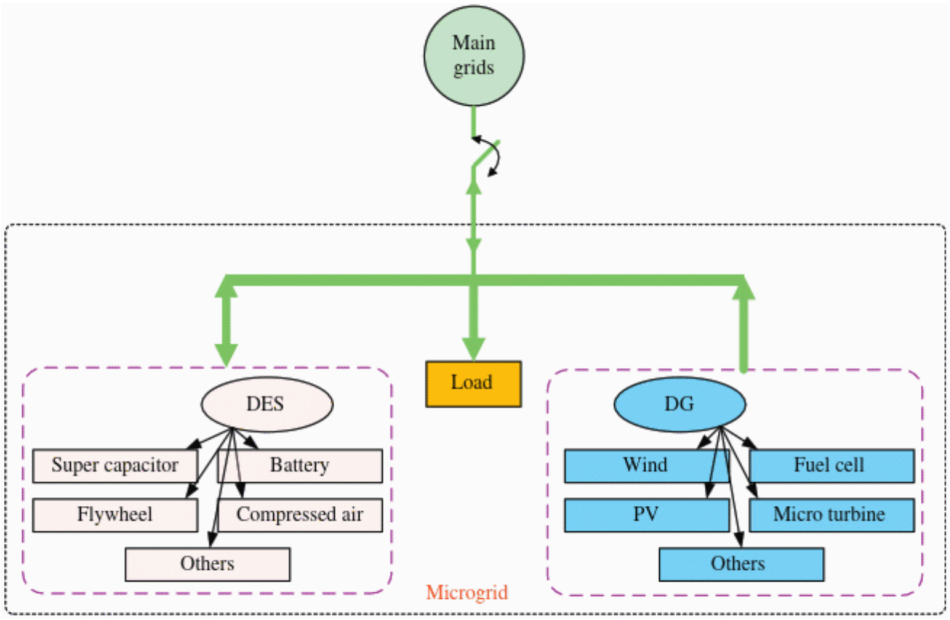

Figure 1.2 Typical structure of a microgrid [9]

The technology for distributed generation (DG) is maturing and increasingly used in the power grid. In addition, many countries have taken a positive attitude towards the development of microgrids, due to problems like the depletion of natural resources, fluctuating fossil fuel prices, and security of supply. There are already some examples of the added value of microgrids today, be it the power supply on Kodiak Island in Alaska, Puerto Rico, Landau in Germany or one of the most popular microgrid projects in Brooklyn, New York [7]. It can be foreseen that microgrids will play an essential role in future electric power and energy systems [9]. The conceptual differences between the traditional grid and a grid including microgrids can be seen in Figure 1.3 Figure 1.4 [10].

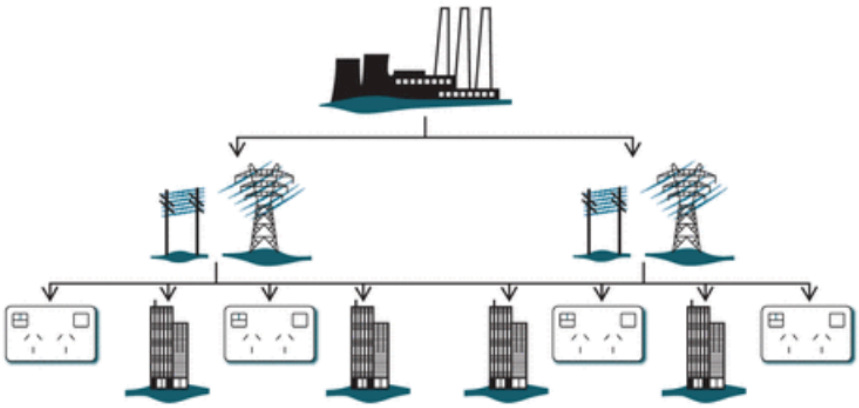

Figure 1.3 Traditional grid [10]

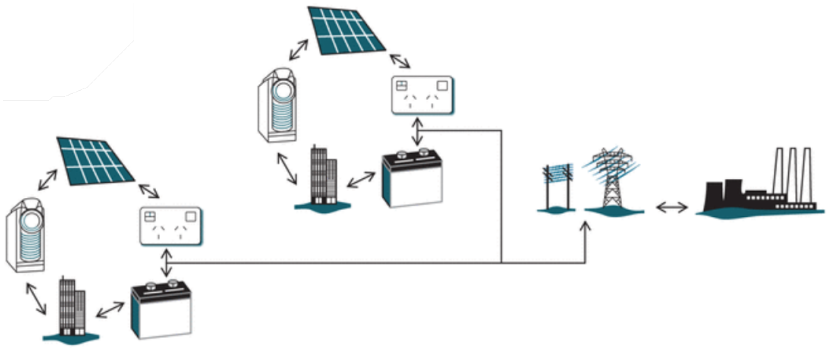

Figure 1.4 Microgrid [10]

1.1.1 Typical topologies

Regarding microgrid topologies, they can be categorised in three major groups: AC, DC or hybrid microgrids. The basic concepts of these types and operation modes are described below.

AC Microgrids

The concept of typical AC microgrids consists of DGs (PV, wind turbines, fuel cell etc.), an AC switch (ACSW), battery and a bidirectional converter, which is depicted in Figure 1.5 [11].

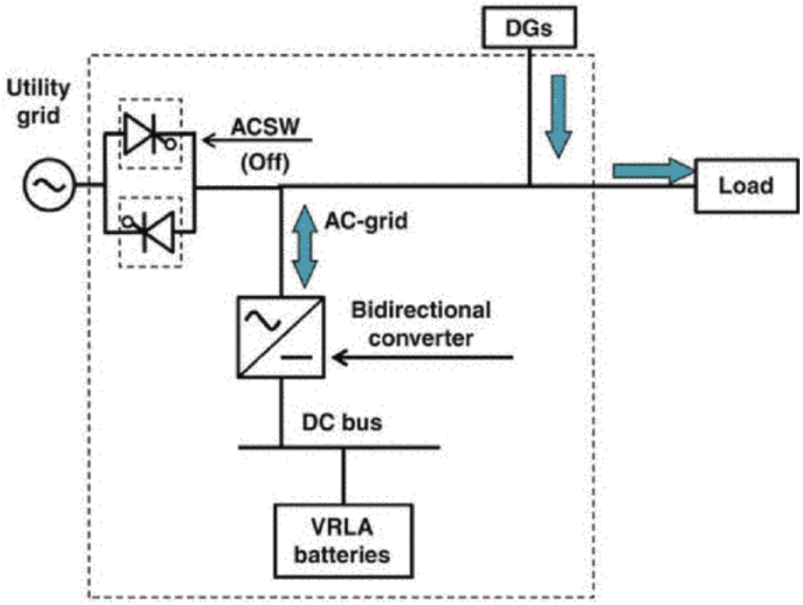

Figure 1.5 Basic concept of AC microgrid [11]

Between the utility grid and AC grid is the ACSW inserted, this allows the system to switching between operation modes. The AC grid is also connected to the DGs and the bidirectional converter, where the converter is connected to a battery via a DC bus [11]. In addition to the PV systems, an

inverter is necessary, as alternating current flows in the power grid, which, however, is not recorded in the Figure 1.5 before. The loads are then supplied directly via the AC grid.

DC Microgrids

The Figure 1.6 shows the basic concept of a DC microgrid consists of PV generation system, DC/DC converter, a bidirectional converter, storage batteries, DC load (for example LED light, LED television, air conditioning etc.) and AC loads (for example hairdryer). The PV system is connected through a DC/DC converter to the DC bus. The generated DC power is supplied to the DC loads, batteries and bidirectional converter. The AC loads are supplied by the bidirectional converter [11].

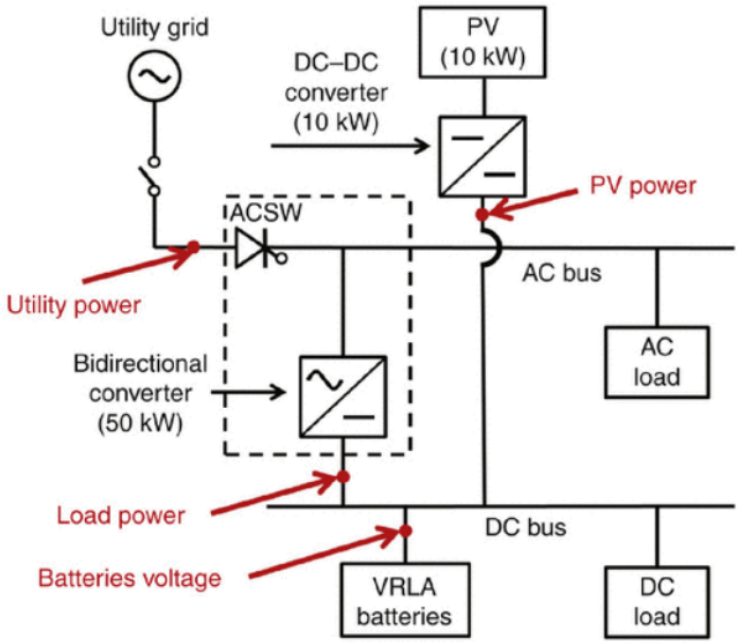

Figure 1.6 Basic concept of DC microgrid [11]

The Figure 1.7 compares the two AC and DC. It is recognisable that the use of DC power supply can reduce the number of AC/DC converter, as shown in Figure 1.7. Because the DC distributed system can work without a DC/AC converter and can supply directly the DC loads. The AC loads are supplied by the bidirectional converter, which can lead to improve power distribution reliability and power quality [11]. Furthermore, the AC loads can be connected directly to the AC grid, but this will be showing a typical architecture of a hybrid microgrid system than a DC distributed system (Figure 1.7), where both AC and DC grids are used.

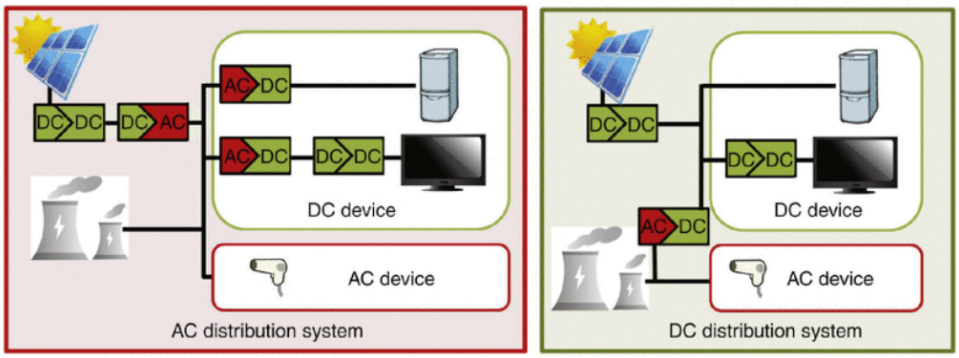

Figure 1.7 AC and DC distributed systems [11]

Hybrid Microgrids

The most common topology for microgrids is the AC microgrid. It provides a direct way to integrate DG units in the current utility grid with little adjustments. Another interesting configuration of microgrids is the hybrid ac/dc microgrid. This topology combines the advantages of both AC and DC architectures, where two networks combined in the same distribution grid (see Figure 1.8). In this case it is possible to integrate both AC and DC based DGs, energy storage systems (ESS) and loads [12].

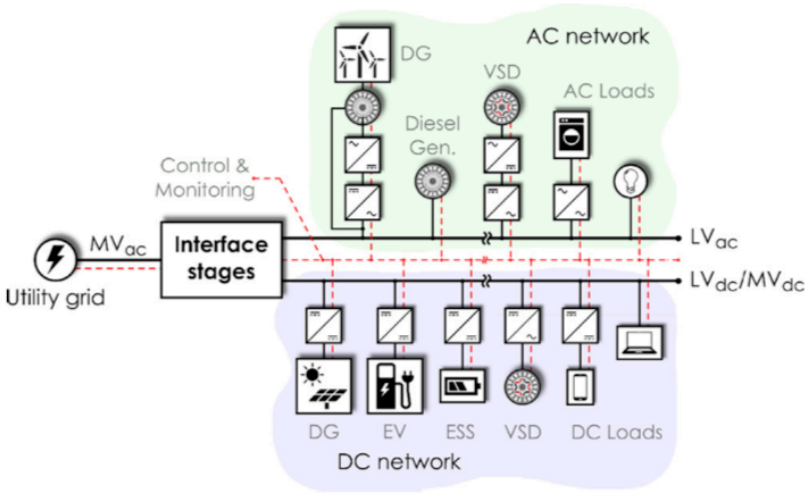

Figure 1.8 Typical system structure of a hybrid microgrid [12]

1.1.2 On/Off grid operation

The systems have two state transitions (see Figure 1.9) and three operation modes (see Table 1.1), which will be explained in the respective chapter.

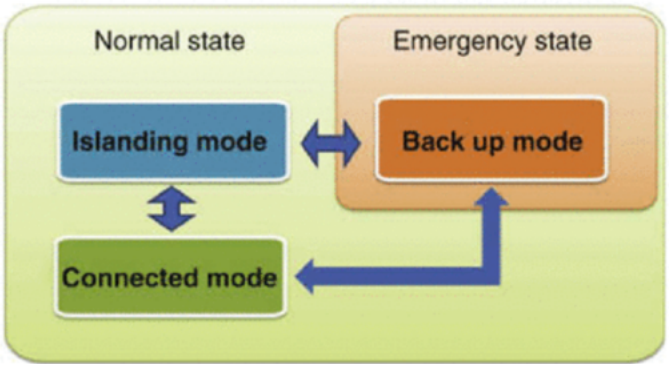

Figure 1.9 State transitions of the system [11]

Table 1.1 System Operations Modes

Mode	ACSW
Islanding	OFF
Connected	ON
Back up	OFF

The shown operation modes in Table 1.1 will be explained in following for an AC microgrid topology and later on for a DC microgrid.

AC Microgrid operation behaviour

The islanded or off-grid mode is a system which operates without being connected to the utility grid and only with energy storage systems and DGs, by turning off the ACSW [11].
When the system operates in the on-grid mode, it is connected to the utility grid. The PV system generates electricity, which is fed into the utility grid. Thus, the PV system is used to supply the consumer parallel to the public grid. To avoid large transport losses, the decentralized solar energy is produced close to the consumer [13].
It is also possible to use photovoltaic systems alternative to the utility grid. The system is connected to the grid and close to the consumer but instead of feeding the surpluses produced electricity into the power grid, they are primarily stored in an energy storage. This is often used as so-called backup system in weaker supply networks or in off-grid mode to ensure better supply reliability. The connected systems are more common in industrialized countries, whereas backup systems are used more in emerging or developing countries [13].

DC Microgrid operation behaviour

In off-grid mode, the DC loads are supplied by the PVs and the AC loads by the bidirectional converter. In case of lower load power demand than generated power, the surpluses will be used to charge the storage devices.

If the power consumption of the loads is higher than the power supply of the PV, the storage batteries provide power through the bidirectional converter by the amount equal to the power shortage (back up mode). The storage batteries will be discharged until there is a shortage of stored energy, after which the system will switch to the on-grid mode to charge the batteries [11].

Some of the advantages and disadvantages of these different topologies are demonstrated in Table 1.2.

Table 1.2 Advantages and Disadvantages of microgrid topologies [12, 14]

Topology	Advantages	Disadvantages
AC microgrid	• DGs are integrated with little effort into current utility grid • Similar to conventional system; therefore, it is possible to apply conventional power system operational concepts for e.g. power flux control, protection devices, fault detection etc.	• Need for synchronization of DGs • Control and operation are difficult
DC microgrid	• No need for synchronisation of DGs • Absence of frequency and phase dependences among AC generators. Converters in DC microgrids are mostly DC/DC or AC/DC	• Higher initial cost due, in part, to unfamiliarity of the system • General lack of code recognition and efficiency metric recognition leading to difficult certification and code compliance.

	• Higher overall efficiency →less interface converter and no circulation of reactive current in network	
Hybrid microgrid	• Integration of the increasing DC-based units e.g. PV, fuel cells, ESS, laptop mobile phones, etc. • No need for synchronization of generation and storage systems → are directly connected either to AC or DC grid • Voltage transformation: modification of voltage levels can be performed in: - AC-side by transformers - DC-side by DC/DC converters	• Protection devices for DC-based networks have not been researched so deeply compared to AC-based networks • Lower reliability than in AC microgrids, as an interface power converter is introduced in the network to generate the DC-link. • Management of hybrid microgrids is more complex, as the devices connected to the AC and DC grids and the interface power converters must be controlled between them

1.2 Storage technologies

The importance of storage technologies and their reliability, as well as the resulting improved operability of microgrids, was already evident in the previous chapters. This chapter will describe different storage technologies in a microgrid system.

1.2.1 General storage technologies

The main function of energy storage devices in a microgrid is to take care of the balancing between power and energy demand with the generated power [15]. Particularly in islanded mode, where there is no connection to the conventional network, the generated power from DG units cannot be

instantly matched to load demands. Therefore, the inclusion of ESS is an important aspect, which allows compensation of unbalances and ensure quality of supply. For this the required amount of power for balancing the system disturbances and significant load changes must be provided by the ESS. The intermittency of renewable energy sources (RES) will be also be mitigated, whereby ESS can be provided additional power on request [16]. Furthermore, the transition between islanded and connected mode is running seamlessly by ESS. Due to establishing optimal periods to interchange power with the distribution grid during the connected mode, power and energy requirements of microgrids are supported by ESS, which is raising the overall performance of the system [16]. ESS are general divided into mechanical, electrochemical, chemical, electrical and thermal storage systems (see Figure 1.10).

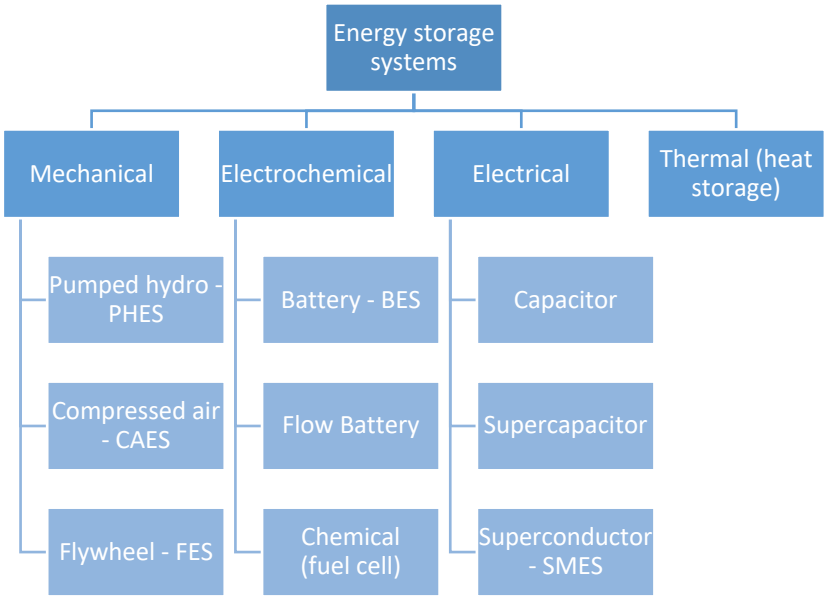

Figure 1.10 Classification of energy storage systems [9]

There are many systems that have been developed for large-scale-energy storage purposes, such as compressed air (CAES) energy storage facilities, pumped hydro (PHES) as well as flywheels, superconductor magnetic energy storage (SMES) and capacitors. Most of them are limited in their site dependence, response capability or capacity. Electrochemical energy storage technologies offer the flexibility in siting, capacity and rapid response required to meet application demands over a much wider range of functions than many other types of storage. Battery energy storage systems (BESSs) have a long history of being integrated into the grid and have great growth recently due to their high energy density, versatility and efficiency [17].

This work will focus on the battery management system of an AC microgrid, based on only PV system, in off grid mode. Therefore, in the next chapter, only electrochemical storage systems will

be explained. Later on, in this work a flywheel model will be integrated to the battery-based system for high current and short-term load levelling to reduce charging cycles and high currents for the battery storage for reduced cyclic aging. The used flywheel model will be discussed and explained in Chapter 2.2.3.

1.2.2 Electrochemical storage systems

In the following, an overview is provided of the electrochemical storage system, where electrical energy is stored as chemical energy.

Lithium-ion battery:

In the last couple of decades, Lithium-ion batteries have been used in consumer products, but due to their combination of high energy and power density, they are increasingly favoured in hybrid/full electric vehicles and large-scale energy storage [18]. As a result, if gasoline-powered vehicles are replaced by electric vehicles, lithium-ion batteries can reduce greenhouse gas emissions. Likewise, because of their high energy efficiency, they can be used in various power grid applications that contribute to improving the quality of decentralized generation systems (wind, solar, etc.). This, in turn, will create wider use and a more energy-efficient economy [19].
Lithium-ion batteries consist of a graphite anode, a lithium metal oxide formed cathode (e.g. $LiCoO_2$, $LiMO_2$, $LiNiO_2$ etc.) and an in an organic liquid (e.g. $LiPF_6$, $LiAsF_6$, $LiClO_4$ or $LiBF_4$) dissolved lithium salt existing electrolyte, to be able to reversible fit in ions and electrons [20]. Depending on the used organic liquid, the life expectancy as well as the specific electrical performance of the lithium-ion battery can be influenced [18]. A typical structure of a lithium-ion battery energy storage system (BESS) including charging and discharging processes is shown in Figure 1.11.

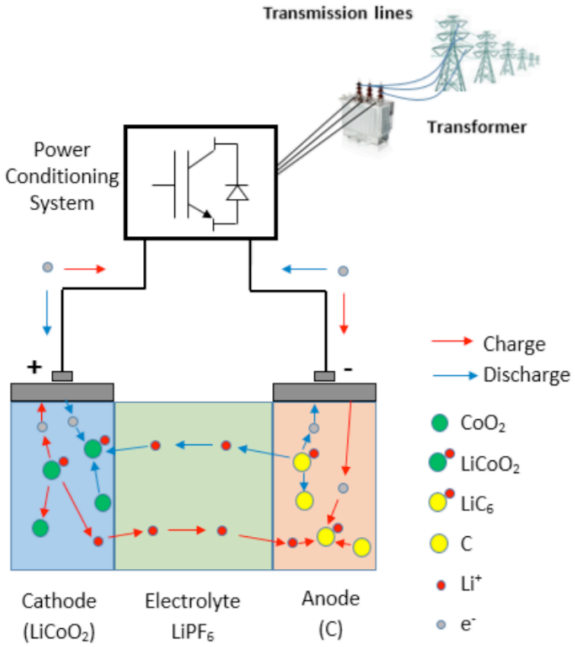

Figure 1.11 Schematic diagram of Lithium-ion BESS [20].

During charging processes lithium ions migrate from the positive electrode to the negative, this process will be repeated in reverse during discharging phase.

Lead-acid battery:

Lead-acid (Pb-acid) is the oldest rechargeable battery system. The Lead acid battery is rugged, is economically priced and delivers bulk power cheaper than other types of batteries. The battery is the preferred choice for automobiles, golf cars, forklifts, marine, hospital equipment, wheelchairs, personnel carriers, emergency lighting and uninterruptible power supplies (UPS) [21]. The operation of a Pb-acid battery is shown in Figure 1.12.

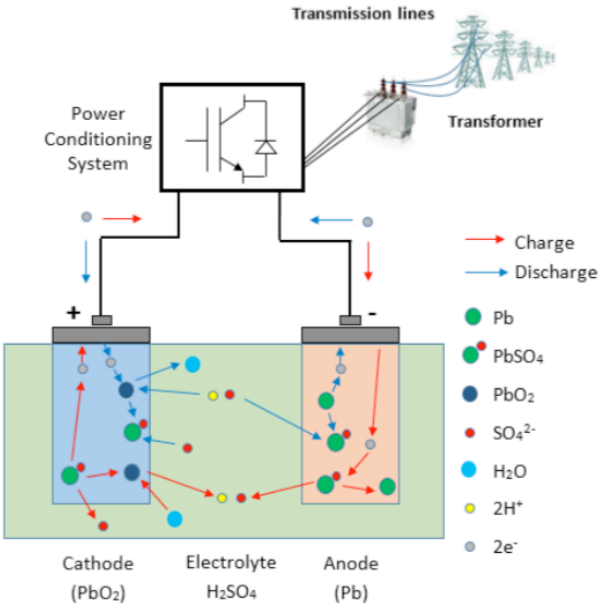

Figure 1.12 Schematic diagram of Pb-acid BESS [20].

The battery consists in the charged state of lead (Pb) and lead oxide (PbO2) both in 37% sulfuric acid (H2 SO4). During the discharged state, as well as at the anode and cathode lead sulphate (PbSO4) is produced, while the electrolyte changes to water [20].

Flow battery:

Flow batteries convert electrical energy into chemical potential, where conventional batteries store energy in solid state electrodes. The flow battery consists of the components stack cell, storage tanks and flow system (see Figure 1.13). The electrolytes (catholyte and anolyte) of the battery are stored in the fluid tanks. Due to the circulation the system reacts in the cell upon operation. The electrolytes are pumped during charging and discharging through the stack cell. The stack cell determines the power, while the size of the tanks determine the capacity and the stored energy. This makes it possible to meet different requirements regarding the independent control of the overall capacity and power. There are three types of flow batteries: vanadium-redox (VRB), zinc-bromine and polysulfide-bromine [22].

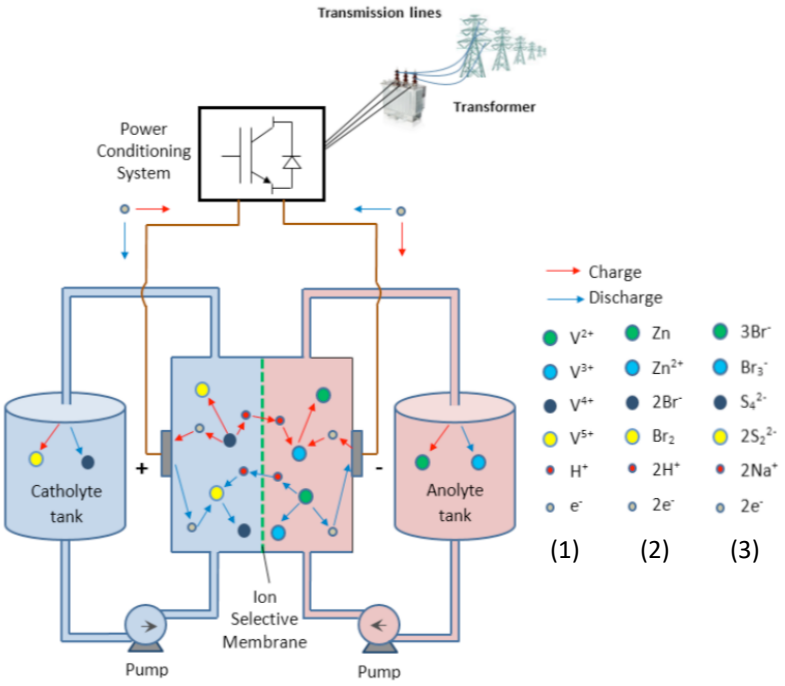

Figure 1.13 Schematic diagram of vanadium redox (1), zinc-bromine (2) and polysulfide-bromine (3) flow BESS [20].

Chemical (fuel cell):

Fuel cells combine hydrogen (H) and oxygen (O) to produce electrical power without emission of any environmentally damaging pollutants such as CO_2. Producing electricity via H_2 is realized through fuel cells. The reaction of hydrogen gas with the oxygen of air is providing electricity and water, which can be recycled and reused to produce more hydrogen. The charging process works vice versa: Hydrogen is produced by splitting water through electrolyzes into its simplest components H_2 and O_2 [23].

1.3 Battery Storage Systems

1.3.1 Evaluation parameters

The evaluation of the battery storage systems is based on some parameters, which are listed and explained below in Table 1.3.

Table 1.3 Evaluation parameters [24].

Parameter	Symbol [Unit]	Description
Round-trip efficiency	η [%]	The ratio of output energy to input energy
Energy density	E_v [Wh/l]	Amount of energy that can be stored per unit volume
Specific energy	E_m [Wh/kg]	The amount of energy that can be stored per unit mass. (capacity)
Power density	P_v [W/l]	Ratio between the available power of a system and it's volume
Cycle lifetime	N_{cyc} [cycles]	The max. number of full cycles that can be achieved by a storage system before it fails (end of lifetime according to a specific criterion)
Calendar lifetime	L_{ca} [y]	The lifetime of unused storage system until it fails according to a specific criterion
Self-discharge	S_d [%/month]	It represents the energy loss due to an internal process in the energy storage system
Charge time	Charge [h]	The time needed to recharge.
Response time	Respn. [τ]	Required time to reach the full power of the system since it was requested
Maintenance Requirement	M [frequency]	Time interval needed to maintain.
Power installation cost	C_p [€/kW]	The costs of installing certain amount of output power
Energy installation cost	C_e [€/kWh]	The costs of installing a certain amount of energy capacity

Parameters and Classification of battery storage systems

The battery storage systems, which were introduced in Chapter 1.2, are depicted in Table 1.4, where a comparison based on the evaluation parameter in Table 1.3 is carried out.

Table 1.4 Parameters of battery storage systems [24, 25, 26].

Symbol [Unit]	Li-ion	Lead-Acid	Flow battery (VRB)	Fuel cell
η [%]	85-90	70 – 90	70 – 80	34 – 40
E_v [Wh/l]	200 – 350	50 – 100	20 – 70	n.a
E_m [Wh/kg]	75 – 250	30 – 50	10 - 30	40
P_v [W/l]	100 – 3500	10 - 500	n.a	n.a
N_{cyc} [cycles]	1000 – 5000	500 – 2000	>10000	n.a
L_{ca} [y]	5 – 20	5 – 15	10 – 15	5 – 15
S_d [%/month]	3 – 5	3 – 5	3 – 5	0.9
Charge [h]	2 – 4	8 - 16	overnight	n.a
Respn [τ]	ms	ms	s	min
M [frequency]	low	high	high	high
C_p [€/kW]	150 – 200	150 – 200	1000 – 1500	1500 – 2000
C_e [€/kWh]	300 – 800	100 – 250	300 – 500	n.a

Based on this classification, Li-Ion battery is the only energy storage technology, which fulfils the system requirements regarding calendar and cycle lifetime, efficiency, response time, power and energy density for microgrids and electric vehicles, where they have proved to be the most promising option [24]. Despite the above advantages, the high battery costs are the main drawback of lithium-ion batteries. However, these are predicted to decrease in the future, partially through the use of second-life batteries. Second-life batteries are used electrical vehicle batteries at the end of their useful lives. The electrical vehicle battery will still have 80 percent of its initial energy capacity when it retires from the vehicle, this makes them very valuable and can be used very efficiently as stationary storage for many years. Thus, the cost of Li-ion batteries can be reduced by utilizing a retired electrical vehicle battery and make the investments in microgrids more attractive by shortening the payback time [27].

1.3.2 Reliability

The increase in the demand on batteries requires improvement in battery diagnostics to observe capacity loss to maintain reliability as the capacity drops, to prevent catastrophic failures by identifying anomalies and predicting the end of battery lifetime when the battery fades to a set capacity threshold. Unfortunately, there is no quick method to test them with certainty, because battery is similar to a living organism that cannot be measured and thus according to symptoms the accuracy of testing varies [28].

The energy storage is represented by the capacity, the internal resistance relates to current delivery and self-discharge reflects mechanical integrity. All these characteristics are responsible for the state-of-health (SOH) and must be fulfilled to qualify a battery. Other properties are the different state-of-charge (SOC), charge and discharge events, length of storage, environmentally conditions, aging, temperature and rest periods of a battery, which effects the performance and complicate the rapid-testing. It is not always possible to distinguish between a weak battery pack that is fully charged and a good one, which is partially charged. This both have different performance levels, but similar runtimes. The most common battery test methods are listed on the table below (see Table 1.5) but it should be also considered that reliable measurements are only possible, if robust symptoms are present [28].

Table 1.5 Most common battery test methods [28].

Test Method	Description
Voltage	• Voltage of the battery reflects state-of-charge in an open circuit condition when rested. • The Estimation of battery state-of-health (SOH) cannot be done alone by the voltage.

Ohmic	• Also called impedance test.
	• Measures internal battery resistance
	  ○ to verify loading characteristics and
	  ○ to identify fault conditions.
	• Identification of corrosion and mechanical defects.
	• Anomalies indicate the end of battery life, but resistance readings often do not correlate with capacity

Full cycle	• To read the capacity of the chemical battery by charge/discharge/charge.

	• Providing the most accurate readings and calibrates the smart battery to correct tracking errors
Rapid	'Common test methods include time domain by activating the battery with pulses to observe ion-flow in Li-ion, and frequency domain by scanning a battery with multiple frequencies. Advanced rapid-test technologies require complex software with battery-specific parameters and matrices serving as lookup tables [13].'
BMS	• Battery Management Systems estimating SOC by monitoring voltage, current and temperature. • BMS for Li-ion also counts coulombs. • A BMS can identify a battery defect but is unable to estimate capacity accurately.
Coulomb counting	• Reads in-and out flowing current. • Provided by Full Charge Capacity (FCC) of a battery, Coulomb count relates to • . • The readings can be inaccurate if the battery is not calibrated. • A full cycle corrects the tracking error.
Read-and-Charge	Reading battery SOC with a proprietary filtering algorithm and then counting the coulombs to fill the battery by a charger featuring RAC technology. →Provides this parameter that is stored in the battery adapters. RAC technology is developed by Cadex.
SOLI	• State-of-Life-Indicator • Estimating battery life by counting the total coulombs a battery can deliver in its life. • A new battery starts at 100%; delivered coulombs decrease the number until the allotment is spent and a battery replacement is imminent. • The full scale is set by calculating the coulomb count of 1 cycle based on the manufacturer's specifications (V, Ah) and then by multiplying the number with the given cycle count. • Developed by Cadex • Can be used in in wheelchairs, medical devices, traction and UPS, installed when new or added as retrofit

According to [29] battery lifetime can be prolonged by:

1. Reducing stress by moderate two to three-hour-charge rather than an ultra-fast charge lasting less than one hour
2. Prevent harsh and erratic discharges
3. Better charge a battery more often than draining a battery fully (Depth of Discharge = DoD)
4. Prevent unfavourable temperature conditions – extreme cold and high heat
5. Checking small to mid-sized batteries with a full charge/discharge cycle on a battery analyser[1]
6. Maximising battery life without added risk and cost saving with 10–20 percent spare capacity, which covers at the end of the shift unknowns and emergencies. Done by Cadex battery analysers by discharging before charging

1.3.3 Battery Management

1.3.3.1 Battery Management System

Former Mercedes CEO Dieter Zetsche once said, "The intelligence of the battery does not lie in the cell but in the complex battery system [30]." To enable safe and efficient function while meeting the requirements of different grid applications, the battery storage systems (BESS) need to be controlled properly. Thus, BESSs require a battery management system (BMS) and a system supervisory control (SSC). Battery management system (BMS) is monitoring and maintaining safe, optimal operation of each battery pack, whereas a system supervisory control (SSC) is monitoring the full system [31]. The purpose of a BMS is to provide battery safety and longevity, reveal the state-of-function in the form of state-of-charge (SOC) and state-of-health (SOH) based on the voltage and current measurements. It also provides immediate caution and service in case of high temperature, cell imbalance or calibration. Furthermore, the system indicates end-of-life when the capacity falls below the user-set target threshold [30]. Most of the BMS have only the basic function of protecting the battery and showing the state-of-charge (SOC), which reflects the battery charge level [30, 31]. Figure 1.14 describes a general structure for the implementation of a battery pack and BMS into a BESS.

[1] Battery analyser is measuring the battery capacity and the smart circuit

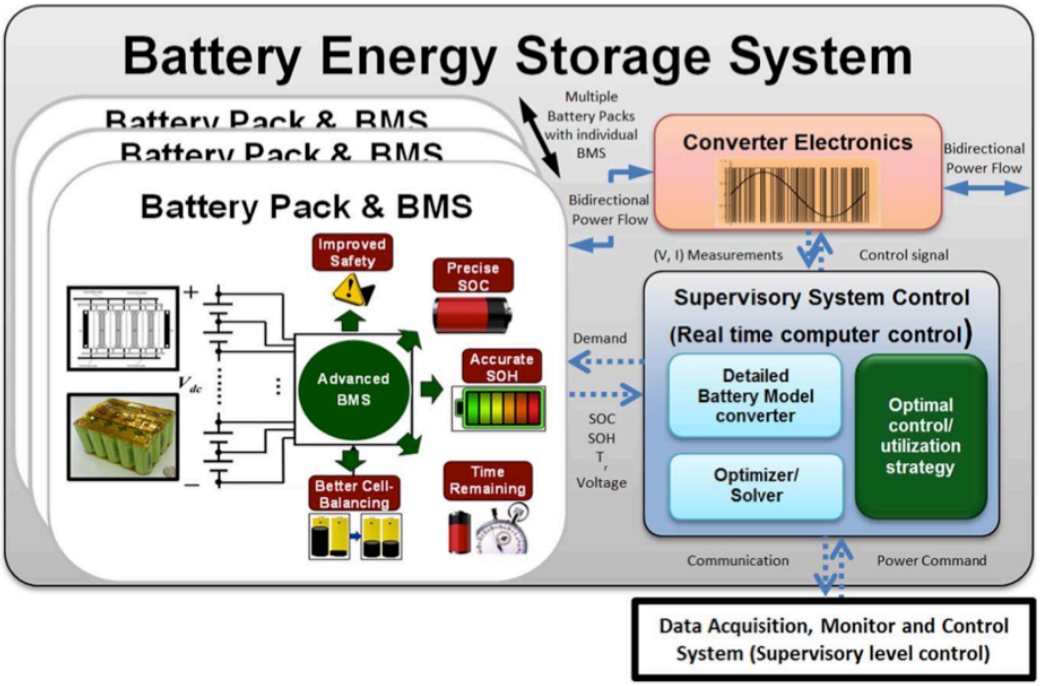

Figure 1.14 Schematic for the implementation of a battery pack and BMS into a BESS [32].

The function of Battery Mode Identification Systems (BMIS) is to determine the mode in which the battery be operated considering SOC as well as the appropriate reference values [33]. The configuration of the proposed battery management system is represented in Figure 1.15.

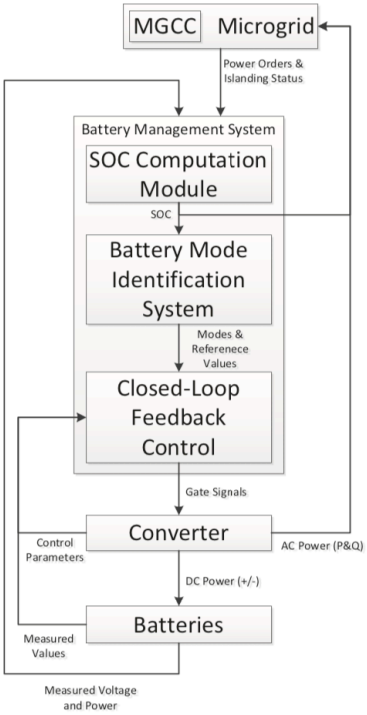

Figure 1.15 Proposed BMS Configuration [33].

The upper operation centre provides the power order and microgrid connection status to the BMS. The BMS also receives measurements from the battery to compute SOC. The SOC computation module is passing the SOC to BMIS to decide if limits are reached and which measures should be taken. The decision making will then be passed by the BMIS to the closed-loop feedback control system which generates PWM gate signals to the converters [33].

1.3.3.2 Battery Energy Management System

The BESSs of microgrids not only require a battery management system (BMS) to provide battery safety, longevity and functioning of the systems, it requires also an Energy Management System (EMS) to maximize the benefit in a microgrid, which is directly related with demand reactiveness and optimal allocation of local energy resources [34]. A typical Energy Management System (EMS) architecture is given in Figure 1.16 that includes forecast, which is needed to uncertainty mitigation of input parameters.

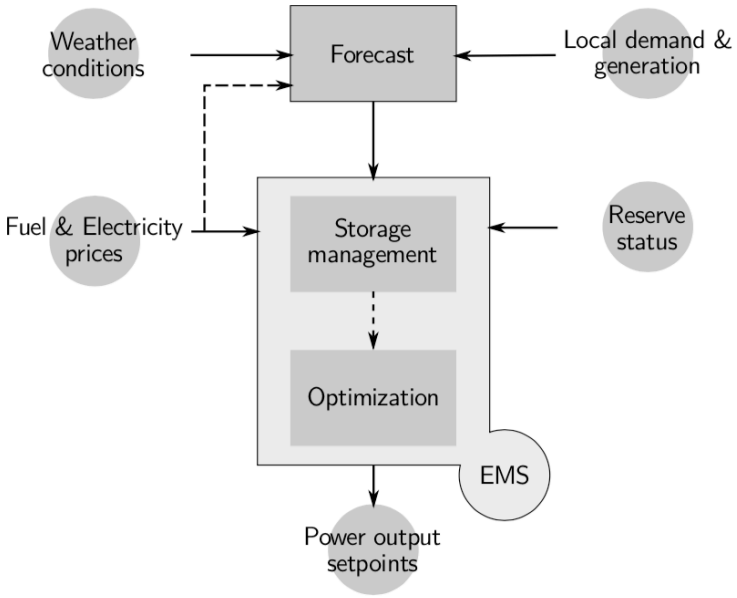

Figure 1.16 Architecture of a typical EMS [34].

The two operation modes of a microgrid, islanded (off-grid) and grid-connected (on-grid) modes, were presented already in previous chapter. During off-grid operation, the main responsibility of the storage is to perform energy balance. During on-grid operation, the goal is to prevent breeding of the renewable source intermittency and load fluctuations to the grid [35].

A sensible element in Energy Management Systems (EMSs) are battery systems because of their performance over its lifetime is highly dependent upon how the battery is operated in real-time during each charge and discharge cycle. Battery life cycle optimization needs to control battery state of charge and charge/discharge rates. In Table 1.6 some approaches are descripted [34].

Table 1.6 Some approaches of EMS [34].

Methods	Description
Rule-based	Changing the constraints (e.g. max. charge/discharge) on the optimization problem depending on the actual state of the battery. This is depending on actual and future (day-ahead) weather conditions.
Fuzzy logic	Using battery state of charge, electricity price, load demand, renewable energy generation, actual solar daily generation and next day solar availability to derive a charge or discharge signal
Charge Management	Charging process of three battery units independently, when one battery is in full condition, the system will disconnect the charging line and two other units keep doing the battery charging process without being influenced by the change of battery. The aims of this concept it to maintain the power balance of PV in order to remain continuously supplies energy at the point of maximum [36].

1.4 Conclusion

In this Chapter different Microgrid topologies and their system operation modes were discussed. Furthermore, the most common battery storage systems for microgrids were reviewed and classified by the evaluation parameters. Microgrids are small power systems that operate independently from the grid and among these storage technologies, the Li-ion is the best-suited storage system that assure reliability and security of power supply for an islanded operation. Furthermore, the battery management system was explained.

2 Object modelling in Matlab

Before developing control strategies, it is necessary to create sufficient models of the microgrid components, which include the battery system, PV module, flywheel and the load profile. The components were modelled as simple as possible in Matlab m.file, but also complex enough to receive adequate data and develop effective control algorithms. Every model was stored in an extra file to make a later change of a model possible, without having to change the whole simulation. All the models need an index to load the specific parameters and the time interval of the simulation. In this way, the models are not restricted to a fixed time basis. After modelling of the appliances, test files were created to check if the typical curves and parameters are verifying correct. These simplified models are based on datasheet values, typical parameters, estimations, databases and previous student work and should be considered as a first basis, which can be used in general and improved for future work.

In the respective chapter the pre-conditions that applied to each model will be explained.

2.1 Battery Model

2.1.1 Review of models in scientific papers

In order to be able to control a battery effectively, a reliable, trustworthy and realistic model of a battery should be created. Batteries are not linear in their behaviour, so it is extremely important that their dynamic responses are known. Li-Ion cells are very complex electrochemical systems due to the coupling between their electrical, thermal and aging dynamical behaviour. These dynamics are determined by the state variables of the cell: SOC, temperature and SOH [24].

The battery model must be accurate enough to fit the dynamic requirements of the application and at the same time it should be as simple as possible [37]. The different model types can be used with different levels of accuracy.

The behaviour of a battery can be fully described by the electrochemical models that capture the chemical phenomena occurring in the battery with equations. However, due to a system of coupled time-varying partial differential equations these models are typically computationally time-consuming. Such models are best suited for optimization of the physical design aspects of electrodes and electrolyte [38]. The mathematical model can predict runtime, capacity and

efficiency by using stochastic approaches or empirical equations. Drawback of this modelling type is that it has no direct relation between model parameters and the I-V characteristics of the battery. Therefore, is has limited value for grid applications [38]. Systems with Li-ion batteries such as microgrids with big ESS (e.g. PV), need to have accurate electrical models of all the components in the system in order to be analysed and optimised. The electrical model represents the battery as an equivalent circuit where the complexity of the model is defined by the numbers of elements in the circuit. The dynamic behaviour of the battery can be modelled with high accuracy by using resistor and capacitor (=RC) in parallel and therefore in the following work the electrical modelling of a battery will be used [38].

2.1.2 Description of the model

The following simplified battery storage model was created using Matlab m.file to be able to follow better their dynamic responses and is based on approximation and datasheet values [39, 40, 41]. First, the typical parameters of the selected battery type were loaded (see in Appendix 1, Table A1.1) to obtain later on the dynamics of the battery. The inputs and outputs of the battery model are chosen as in [24]. For simplification the battery internal temperature, prediction of the output voltage, estimation of power loss as well as the aging of the battery were neglected. The inputs and outputs defined are as follows:

Table 2.1 Battery model inputs [24].

Model Inputs	Definition
Model	Selected battery type/model
Ibatt	Battery current [A]; Discharge: –Ibatt; Charge: +Ibatt
Tamb	Ambient Temperature, will change from 40 to -20 °C, (it is assumed that the cell's initial temperature is equal to ambient temperature 20°C)
SOCinit	initial relative state of charge SOC is =0 when cell is empty; SOC is =1 when the cell is full; SOCinit = 1
dt	Length of time step; 1/60 [h] = 1min
Cbatt	Battery capacity, specific to different battery types [Ah]

Table 2.2 Battery model output

Model output	Definition
SOC	SOC changing by the time step

SOC of the battery is considered as the most important parameter, which reflects the battery performance. The accurate estimation of the SOC can not only protect battery, prevent over discharge, and improve the battery life but also allow the application to make rational control strategies to save energy. A battery is a chemical energy storage source, and this chemical energy cannot be directly accessed, which makes the estimation of the SOC of a battery difficult [42]. However, in general the SOC of a battery is defined as a ratio of remaining capacity to its nominal capacity, where the nominal capacity is given by the manufacturer and represents the maximum amount of charge that can be stored in the battery [39, 42]. The equation of the model is the following:

$$SOC(t) = SOC_{init} + \int_0^t \eta \times \frac{I_{batt}(t)}{C_{batt}} \times dt \tag{2.1}$$

where $SOC(t)$ – battery state-of-charge at time t

SOC_{init} – battery initial state-of-charge

I_{batt} – charge /discharge current, A

C_{batt} – battery capacity, Ah

η – efficiency, defined as the ratio of discharging capacity to the charging capacity

t – time, h

Where I_{batt} is positive if the battery is charging and negative if discharging. The maximum charging and discharging currents depend on the battery's capacity and on the temperature.

All batteries are affected by self-discharge. The different self-discharge rates of different battery types as discussed in chapter 1.3.1 are not a manufacturing defect but a battery characteristic [43]. The self-discharge rate of Lithium-Ion battery is about 5 percent in the first 24 hours and then loses 1-2 percent per month. Under normal circumstances, the self-discharge of Lithium-Ion is reasonably steady throughout its service life, but full state-of-charge and elevated temperature causes an increase. Table 2.3 displays the change of self-discharge rate per month of Li-ion with rising temperature and state-of-charge [43].

Table 2.3 Self-discharge per month of Li-ion at various temperatures and state-of-charge [43].

State-of-charge	0°C	25°C	60°
Full charge	6%	20%	35%
40-60% charge	2%	4%	15%

The values above are estimated with linear function approximation to be able to include them in the battery model. Due to different state-of-charge the linear function was expand with some factors and interpolation.

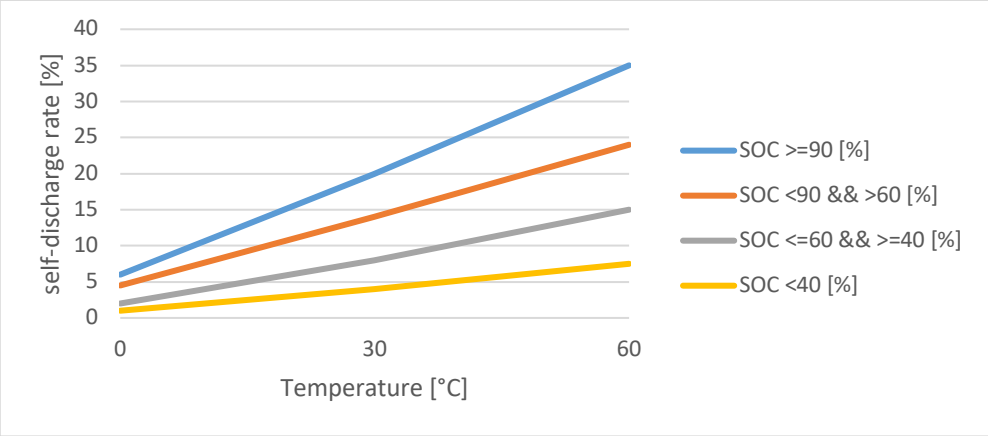

Figure 2.1 Approximation of self-discharge rate at different temperature and SOC

The self-discharge of the battery is calculated as follows:

$$s1 = T_{amb} \times m + c \tag{2.2}$$

$$m = k \times SOC \tag{2.3}$$

$$c = l \times SOC \tag{2.4}$$

Where $s1$ – self-discharge proportion depending on the temperature and SOC

T_{amb} – actual ambient temperature, °C

m – slope at various SOC

c – is the y-value in which the line intersects the y-axis

k – estimated slope of the linear approximation, %

l – estimated factor where the line intersects the y-axis, %

The self-discharge values above are given monthly but were converted to minute values in the model. The total self-discharge rate of the battery model is described as

$$dSOC = -\big(\big(s1 + (s2 \times SOC)\big) \times dt\big) \tag{2.5}$$

Where $dSOC$ – total self-discharge rate of the Lithium Ion battery

$s1$– self-discharge rate depending on temperature and SOC

$s2$ – self-discharge rate of Lithium-ion battery in the first 24 hours

dt – time step

This is included as a function in Matlab, where the specific self-discharge rate will be chosen depending on the current temperature and SOC value (see Appendix 2).

With rising temperature not only, the self-discharge will be affected but also the aging of the maximum charge storage capacity, which should also be considered in the battery model. In [44] represented capacity retention at different temperatures has been adjusted for the used battery model (see Figure 2.2).

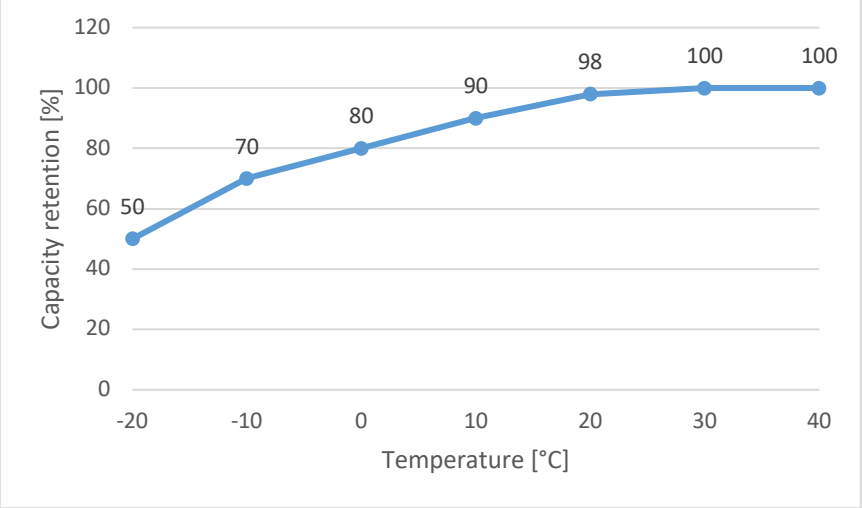

Figure 2.2 Capacity retention at different temperature [44].

Also, the maximum available storage capacity is defined as a function in Matlab, where the input is the current ambient temperature and output the maximum available capacity. The current capacity retention will be chosen by the current ambient temperature, which is computed in Appendix 3. The Matlab file for the battery model is called “Battery_model.m” (Appendix 4).

The complete Matlab code structure of the simplified battery model is illustrated in a block diagram below (see Figure 2.3).

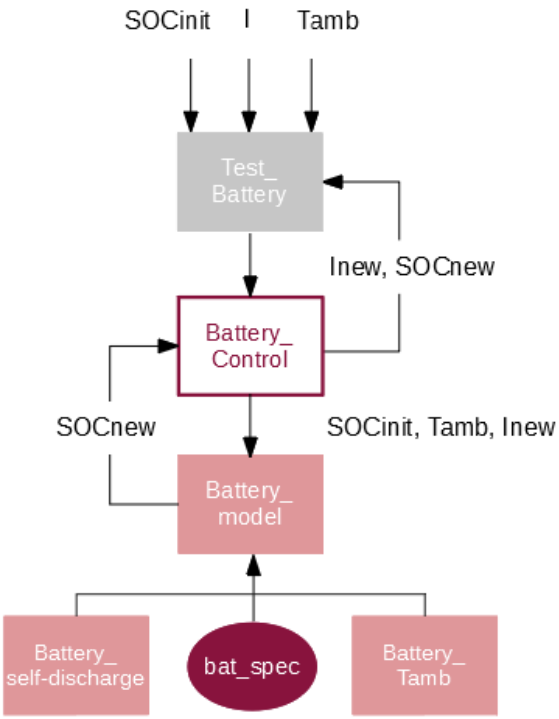

Figure 2.3 Matlab code structure of the battery model

The test file "Test_Battery" created to check key parameters and visualize typical curves of the battery model is setting the initial values, such as SOC_{init}, current ambient temperature (T_{amb}) and the charge/discharge current ($I = I_{batt}$). These values will be called by the file Battery_control.m, which is fixing the new current due to the conditions, such as ambient temperature and state of charge of the battery. Detailed description of battery control strategies will be discussed in Chapter 3.1. The new SOC of the battery is calculated then in file Battery_model.m, which is calling the files Battery_self-discharge.m and Battery_Tamb.m, where the capacity retention and self-discharge values of the battery were settled. This value will be returned to the Battery_control.m and to Test_Battery.m, where the SOC values will be saved for the next time step.

Table 2.4 show typical parameters for different types of battery storage systems necessary to implement sufficient models. These parameters are implemented and used in the simulations.

Table 2.4 Parameters of different battery types [40, 41].

Battery	Application	Energy [kWh]	Cbatt [Ah]	Imax [A]	Vmax [V]	Vnom [V]	η
KOKAM-SLPB120255255	Detached house	3.88	75	75	58.8	51.8	0.96
KROS-H-2-222	Settlement	222	300	1200	832	740	0.97

2.1.3 Verification of the model

The first test of the battery model was constructed to check if the SOC of the battery is changing at different currents and temperatures. Therefore, first initial values were set, where SOC_{init} set to 1 (= battery is full charged) and I_{init} is zero (=neither charging or discharging for the first time step). Ambient temperature was varying from 40 °C to -20 °C degrees and the current from -75 A (discharge current) to 75 A (charge current) in 5 A steps at one-minute time step. The results of this test and all other tests are presented with reference to the detached house battery mentioned above. It can be observed that the battery is charging and discharging perfectly with the set control, suggesting that the model is working properly (see Figure 2.4).

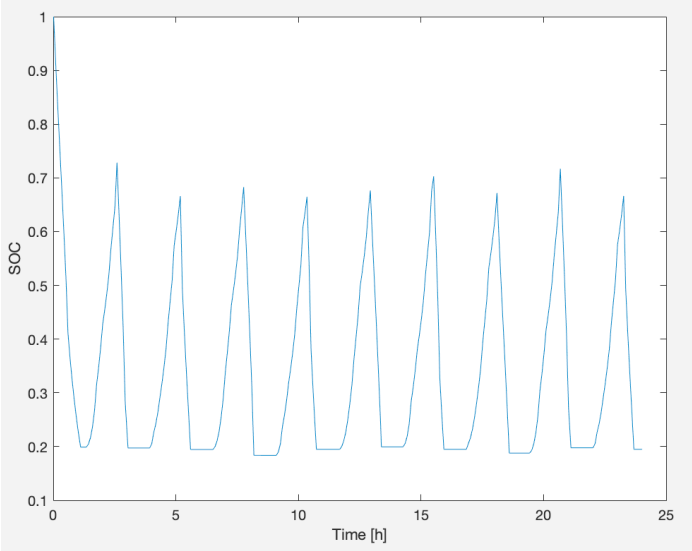

Figure 2.4 SOC behaviour of detached house battery

For the next test, the ambient temperature was set to 20 °C degrees, the initial current to zero and the initial SOC of the battery to full charged. This test will show if the self-discharge effect of the modelled battery is working. As it is presented in Figure 2.5 and also referred in Chapter 2.1.2 the

self-discharge characteristic of the battery is working, the Li-ion battery is showing an self-discharge rate of 5 percent in the 24 hours.

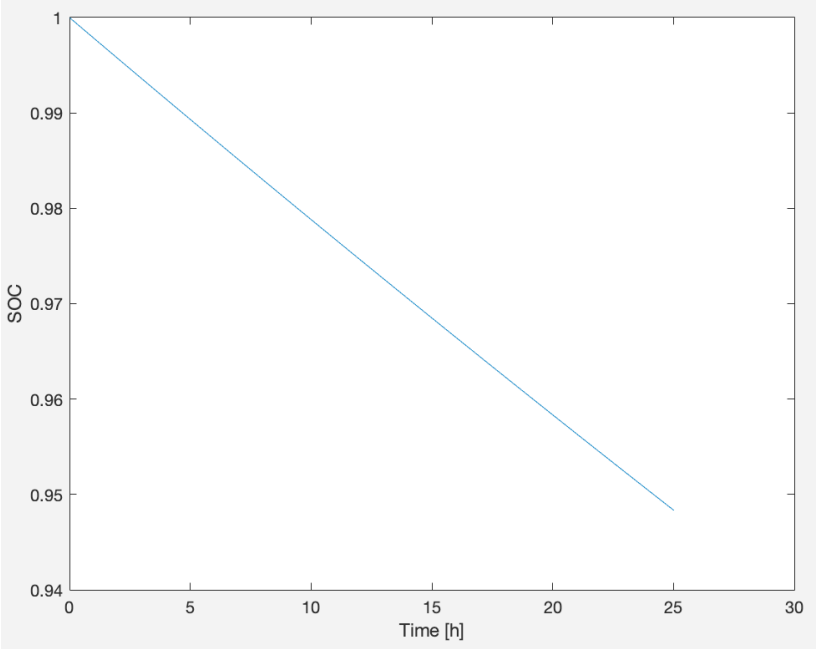

Figure 2.5 Self-discharge effect of the modelled battery

To check the battery efficiency, the battery was discharged until 20 % SOC with 75 A of discharge current and was charged again with 75 A. The calculated efficiency is 90.91 %, which is comparable with the Table 1.4 in Chapter 1.3.

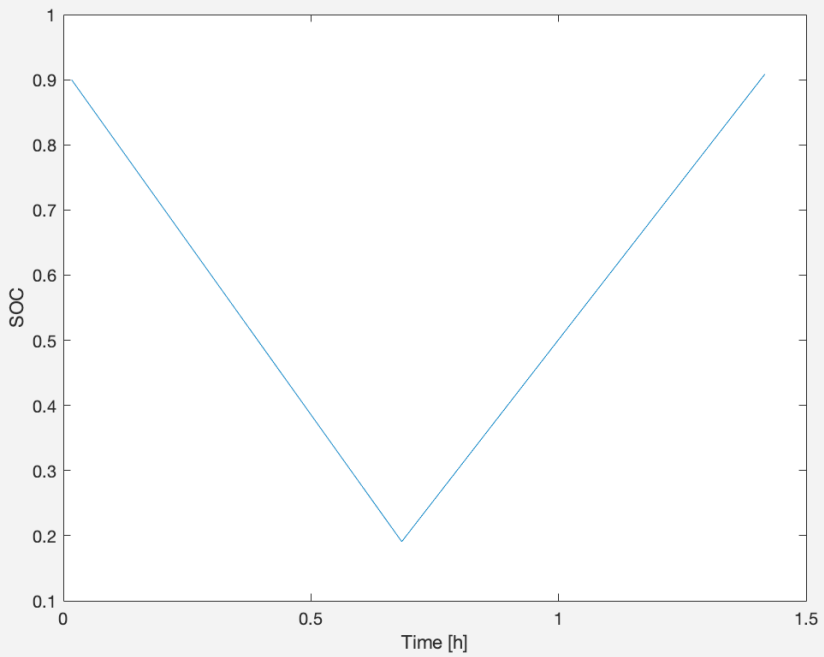

Figure 2.6 Discharge and charge curve of modelled battery

2.2 Other microgrid components

To simulate an islanded microgrid it is necessary to model a PV, load profile and flywheel model. The selected models and datasets used for these models are shown in the following subchapters.

2.2.1 Load profile

The load profiles for different applications such as detached house and settlement were generated with Load Profile Generator software, where appropriate settings could be chosen to generate artificial load profiles [45]. For example, see Figure 2.7, where the load profile of a detached house for one day is simulated. The settings for this simulation are lined up in Table 2.5. See Appendix 6 for the generated load profile of the settlement application as well as their settings.

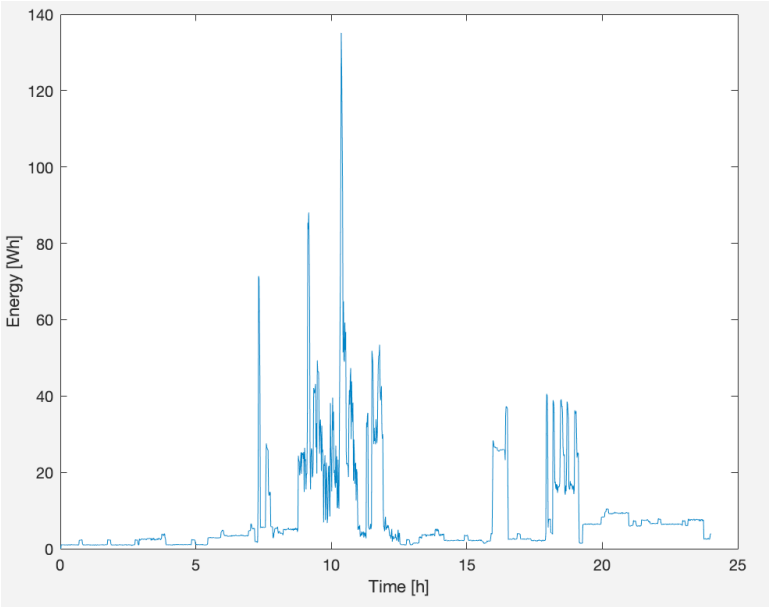

Figure 2.7 Generated load profile of detached house

Table 2.5 Settings overview of a detached house

Overview Household	
People	Family, 2 Children
Size	Normal detached house
Power consumption	3987,97 kWh/ year
Measurement data	Per minute
Duration	1 year

2.2.2 PV System

The PV system is modelled using one-minute measurement data of an existing station. There are 668 PV panels all together with combined output power of 177 kWp. All the panels are divided between 6 inverters - 2 are 20 kVA and 4 are 30 kVA. The Station is located in Laastu Talu OÜ, Nõrava in Estonia. The existing PV plant is too large for particular application such as a detached house or too small for a settlement and therefore has to be scaled accordingly.

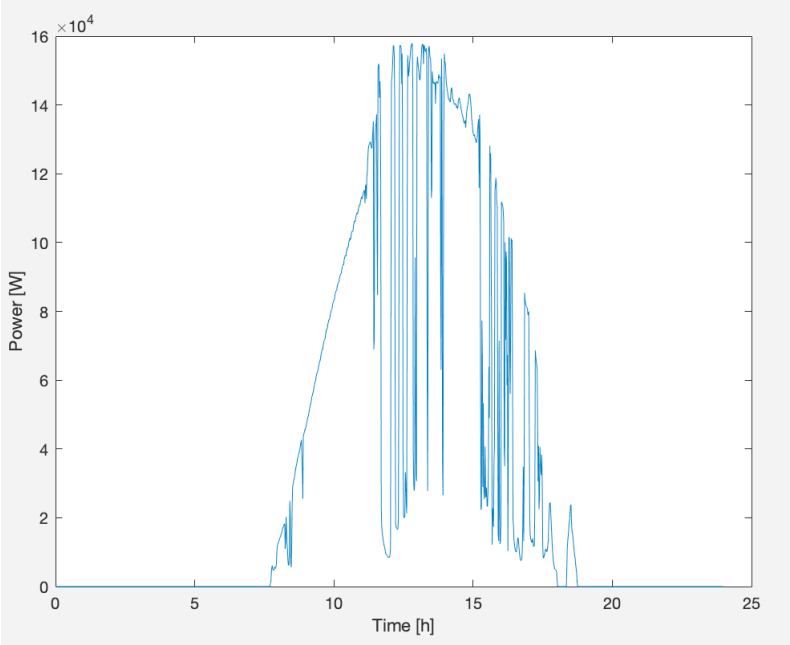

Figure 2.8 Power output of existing PV system

Figure 2.8 pictures the power output of the PV system from 24. Sept. 2018. This is used for an example how the scaling procedure was carried out. Scaling was done as follows:

As an example, the existing PV plant is scaled for a detached house. The design of an islanded PV system is based on the principle that energy production and consumption must be balanced. The decisive factor for the number of solar modules required and system performance is the expected solar radiation [4]. According to the Photovoltaic Geographical Information System (PVGIS) the typical solar electricity generation of Estonia from 1 kWp in country average is about 864 kWh/ kWp [47]. Overview of PVGIS data sources and calculation methods can be found in [48]. To be able to determine the scaling factor, the required power generation for a detached house should be known. For this, the daily power consumption should be calculated. The total power consumption of a detached house was generated by the load profile generator and is 3987.97 kWh/year (c.f.

Chapter 2.2.1) [45]. After determination of the solar electricity generation and the power consumption per year, the minimum required system output can be calculated by dividing the power consumption by the solar electricity generation, which is 4.62 kWp (c.f. Formula (2.6)).

$$Min.required\ PV = \frac{3987.97\ kWh}{864 \frac{kWh}{kWp}} = 4.62\ kWp \tag{2.6}$$

Moreover, a surcharge for certain losses such as battery losses or others should be added on the power consumption, to ensure that the energy demand is covered. Therefore, the PV system should produce at least 25% more power than the household consumes, so the total annual consumption of the household is 4985 kWh per year and 13.66 kWh per day [49, 4]. Thus, the required power generation per day is 819.45 kW, which will be divided by the total power output of the existing PV system and it follows the scaling factor with 0.017. The new minimum required system output after adding the surcharge is 5.66 kWp. All mentioned values are listed in Table 2.6, which gives an overview about all compulsory values to calculate the scaling factor.

Table 2.6 Scaling factor determination of detached house

Power consumption	3987.97	kWh/year
Solar electricity generation Estonia	864	kWh/kWp
Minimum required system output	4.62	kWp
Surcharge for battery losses (25%)	997	kWh/year
Power consumption + surcharge	4985	kWh/year
New minimum required system output	5.77	kWp
Required energy generation per day	13.66	kWh
Total power output of existing PV on 24. Sept.	803	kWh
Scaling factor for 24. Sept.	**0.017**	

As can be seen in Figure 2.9 the power output of the scaled PV system for a detached house. The power output of the scaled system is much lower than the power plant before, which was not suitable for a household. This scaling method is also used for the settlement application (Appendix 5).

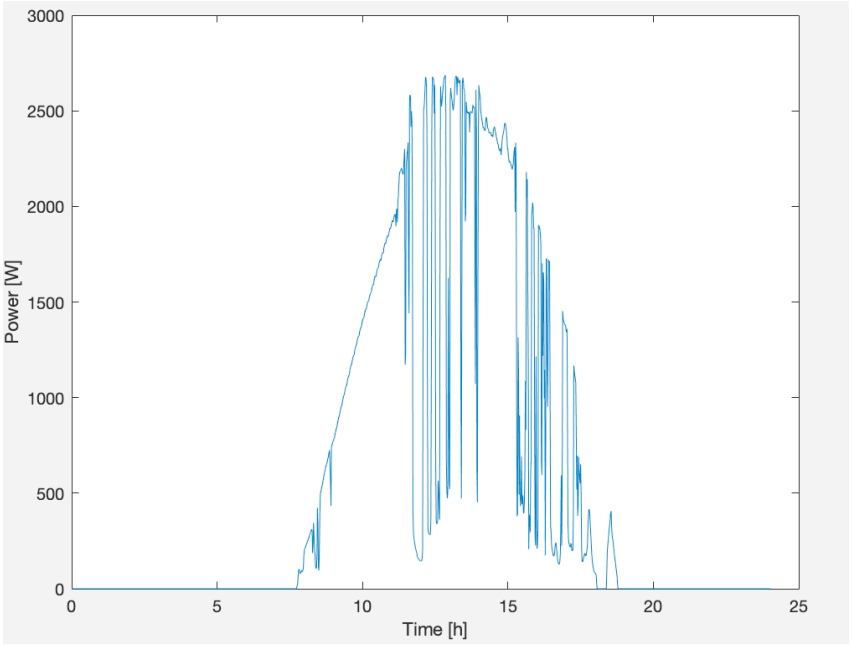

Figure 2.9 Power output of scaled PV system

2.2.3 Flywheel model

The flywheel model is a work of a previous student, which was modeled in Matlab Simulink before and was based on the Rosetta T3-15 flywheel system in the Taltech laboratory [46]. Since this work is based on Matlab m.file, a simplified m.file model of the flywheel had to be created. The previous student work contains too many components and would cause more effort to integrate the flywheel in Matlab m.file. However, the simplified flywheel model is showing the same behavior with a bit error, but this is sufficient to receive adequate data and develop effective control algorithms with the model. For the verification of the flywheel model of a previous student work, a two-minute segment of one second power measurement data of the NRG building in Tallinn University of Technology (Figure 2.10) was used as load profile [46].

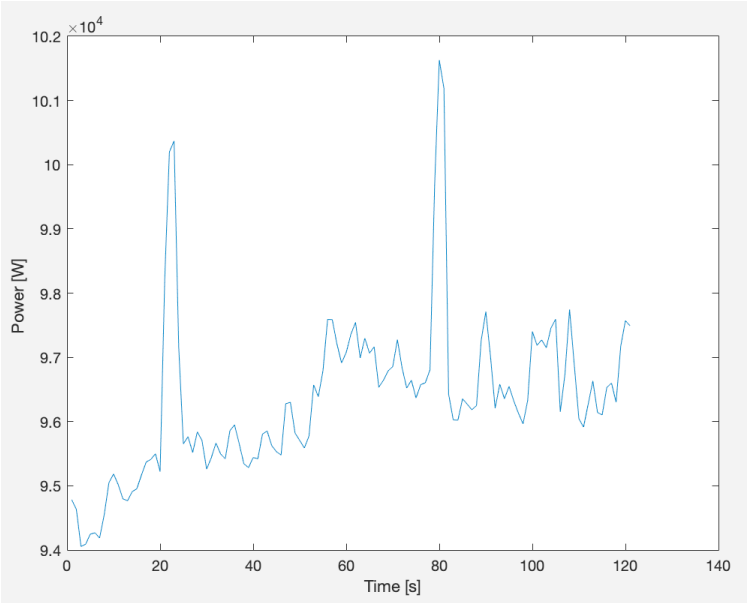

Figure 2.10 Variable load profile used for load levelling

Later one, after verification of the flywheel model, certain load profiles for specific operations were generated. The inputs and outputs of the flywheel model are as follows:

Table 2.7 Flywheel model inputs

Model inputs	Definition
Model	Selected flywheel type/model
Ef	Output energy of flywheel [kWh]
SOCinit	Set SOC value SOCinit=1 (full charged);

Table 2.8 Flywheel model output

Model output	Definition
SOCnew	Returned new SOC value, which changing by the time step

The flywheel model is determining the new state of charge value of the flywheel in the current time step. First the current angular velocity (= w) depending on the current SOC will be computed with the equation (2.7) [50].

$$w = \sqrt{(SOC_{init} \times (w_{max}^2 - w_{min}^2)) + w_{min}^2} \tag{2.7}$$

where SOC_{init} – initial value of SOC of flywheel

w_{min} – minimum angular velocity (lower limit of the usable speed range), rad/s

w_{max} – maximum angular velocity (upper limit of the usable speed range), rad/s

Afterwards angular velocity of the flywheel (= w_f) will be detected with the input parameter Ef, which is defined from the flywheel control model (see Formula (2.8)) [46].

$$w_f = \sqrt{\frac{Ef \times eff \times 2}{J}} \tag{2.8}$$

where Ef – output energy of flywheel, kWh

eff – flywheel efficiency

J – inertia of the flywheel, kgm^2

The newly determined angular velocity (= w_{new}) is the difference between the current angular velocity based on the current SOC value and the angular velocity of the flywheel (see Formula (2.9)), depending if the flywheel is charging ($-w_f$) or discharging ($-w_f$).

$$w_{new} = w - w_f \tag{2.9}$$

where w_{new} - newly determined angular velocity, rad/s

w – current angular velocity, rad/s

w_f – angular velocity of flywheel, rad/s

The resulting new SOC of the flywheel is expressed in equation (2.10).

$$SOCnew = \frac{w_{new}^2 - w_{min}^2}{w_{max}^2 - w_{min}^2} \tag{2.10}$$

where SOC_{init} - flywheel state-of-charge

w_{new} – newly determined angular velocity, rad/s

w_{min} – minimum angular velocity (lower limit of the usable speed range), rad/s

w_{max} – maximum angular velocity (upper limit of the usable speed range), rad/s

The complete Matlab code structure of the simplified flywheel model is illustrated in a block diagram below (see Figure 2.11).

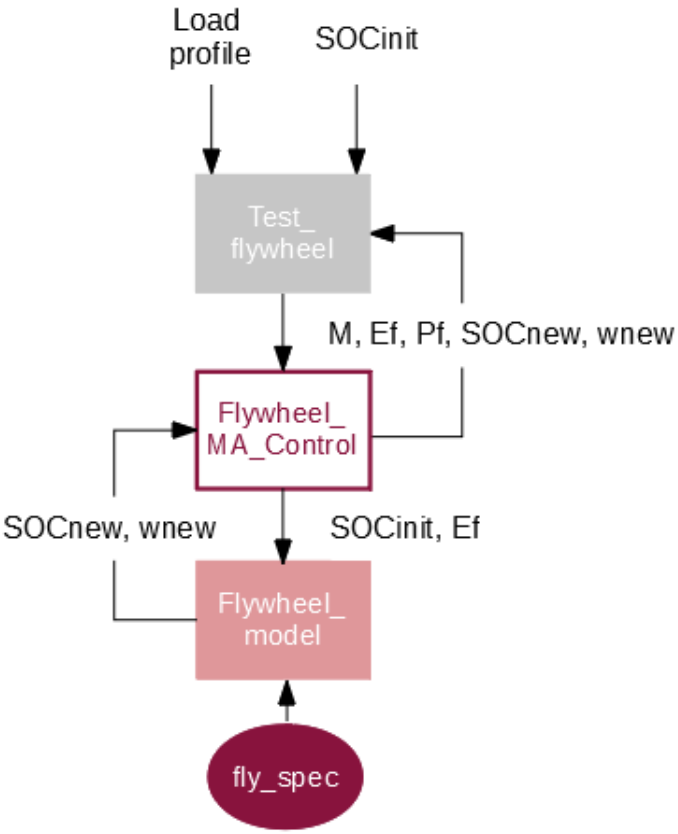

Figure 2.11 Matlab code structure of the flywheel model

The test file of the flywheel model was created to check key parameters and visualize typical curves of the flywheel model, which will be compared with the flywheel model of the previous student work. This file is setting initial values, such as SOC_{init}, which was set to 1 (flywheel is full charged). It calls the simplified moving average (=MA) control model file Flywheel_MA_control.m. This simplified control model was created for verification of the flywheel model. In Chapter 3.2 the moving average control model will be explained more in detail. Furthermore, a custom control model of the flywheel will be considered and compared.

The used MA control model is calculating the output energy of the flywheel Ef, which will be forwarded to the file Flywheel_model, to be able to compute the new SOC value of the flywheel. As well as the different types of battery storage system, also different types of flywheel storages were used to implement sufficient models. These will be chosen by the selected model from workspace file fly_spec. The implemented parameters of specific flywheel types as well as the parameters of the flywheel Rosetta, which was used for verification are listed below (see Table 2.9).

The calculated SOCnew value will be returned to the Flywheel_MA_control.m and to Test_Flywheel.m, where the SOC values will be saved for the next time step. In addition, other parameters and values can be passed further to the flywheel control system or to the test file.

Table 2.9 Parameters of different flywheels [46, 51]

Manufacturer	Application	Energy [kWh]	w_{max} [rpm]
Rosetta T3-15	Verification	0.083	6000
Beacon Power	Detached house	12.5	15500
Beacon Power	Settlement	550	15500

To ensure, that to simplified model of the flywheel is working similarly to the flywheel model of the previous student work, the behaviour of the rotational speed was checked. In Figure 2.12 the rotational speed of both flywheel models is presented.

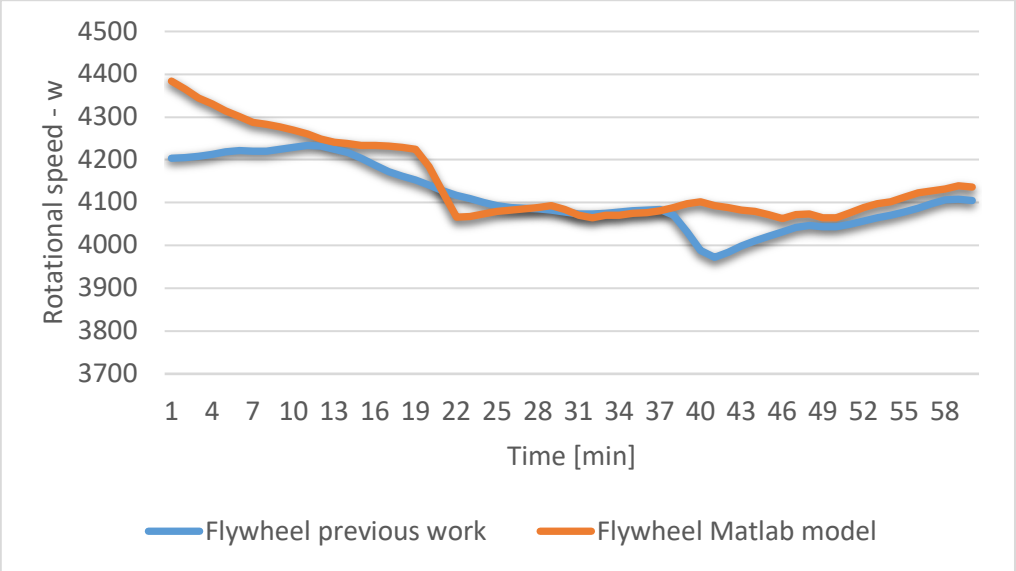

Figure 2.12 Comparison of Matlab and previous student work flywheel model

The performance of the simplified flywheel model was evaluated using the root mean squared error (RMSE) value, which describes the deviation between the modelled flywheel and the flywheel from previous work [46]. The RMSE value was 59.88 rpm, 2.6 % in percent. The flywheel model is working successfully and adequate to intergrade it to the whole system.

2.3 Complete system

To achieve a simpler and clearer structure, all previously described models were combined into one file called Microgrid_model.m (Appendix 7). This object model is retrieving the control models of battery and flywheel storage systems as well as the measurement data of the PV system and load profile. The connections between all components will be assumed as ideal and thus losses have not been considered. The working principle of the temporary islanded microgrid system is shown in the schematic in Figure 2.13.

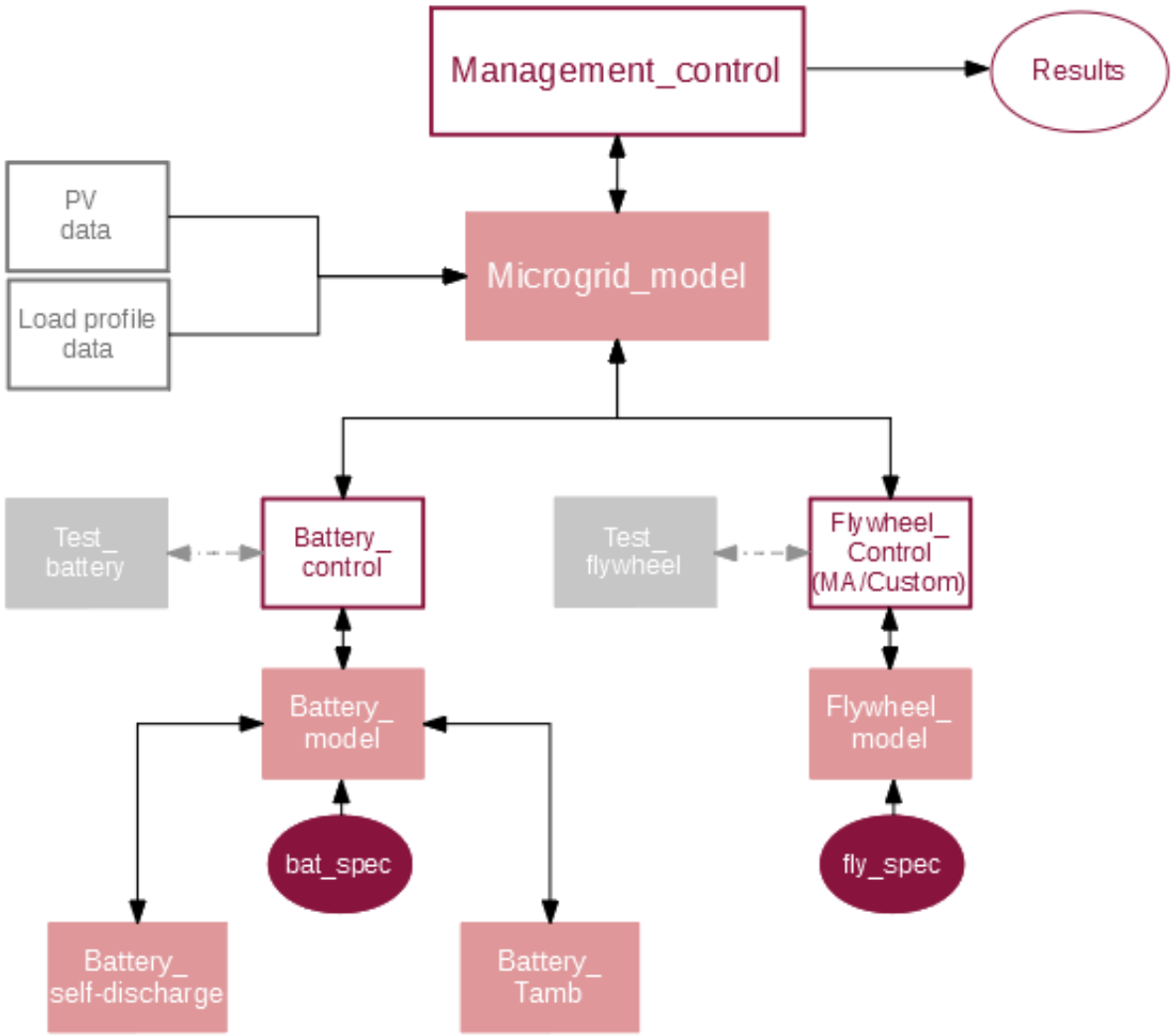

Figure 2.13 Matlab code structure of microgrid system

The microgrid model is forwarding the commands for example, charging or discharging several storage systems, from the Microgrid_control to the certain models. Input and output parameters for the Microgrid_model.m in turn are variables of the individual models, which are relevant for the control purposes in Microgrid_control.m. These values are the power and current of the

components and can be used to determine the microgrid voltage. All the other constant variables are yielded by a parameter file. The flywheel can be activated according to the selected scenario (Chapter 3), which can be also deactivated by setting their x variable to “0”. This skips the calculation of the model completely and only the activated battery storage system will be considered in the microgrid system.

Since the following work is based on an islanded microgrid the mains voltage is considered to be kept constant in any case. According to standardization within the European Union the mains voltage range is nominally at 230 V (V_eff) $\pm$ 10% at 50 Hz [52] and cannot be exceeded. It is assumed that the PV system includes an inverter, which is controlling the exceeding voltage and keeps the voltage constant.

Finally, the voltage will be calculated. The AC current values of consumers, including the battery during charge operation, are calculated. Then the power of all energy producing components is added, including the battery during discharging, and divided by the AC current value to obtain the system voltage. This value will be returned then to the microgrid control, where the values will be saved for each time step and used for the purpose of analysis.

3 Control models and strategies of microgrid system

As stated by the title of this thesis the goal of this work is to development simplified control strategies for energy storages in an islanded microgrid to achieve maximum islanded mode operation time. Figure 3.1 gives an overview of the islanded microgrid components, which were used for the scenario simulations in this work. The models of the integrated components were already discussed in Chapter 2. In the following chapters the control model and strategies of the battery and flywheel storage system will be explained in detail.

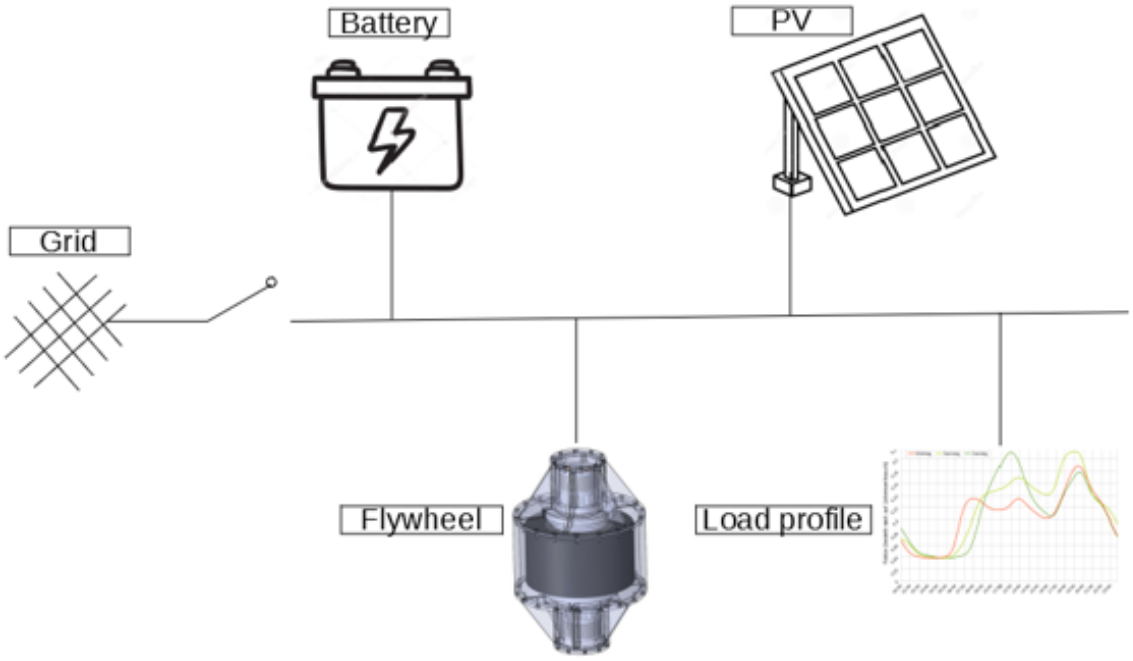

Figure 3.1 Used microgrid model for scenario simulation

3.1 Description of battery control model

In chapter 1.3.3 the importance of the battery management and control system of batteries was described. The battery storage systems need to be properly controlled to be able to ensure safe and efficient functioning while meeting different requirements. The inputs of the modelled battery control are the values set in the microgrid control model as shown in Table 3.1. The control model outputs are presented in Table 3.2.

Table 3.1 Battery control model inputs

Model inputs	
Model	Selected battery type
SOC	Initial SOC of the battery
Ibac	Battery current in AC [A]
dt	Time step [h]
Tamb	Current ambient temperature [°C]

Table 3.2 Battery control model outputs

Model outputs	
Ibacnew	Real AC charge-/ discharge current [A], which set after meeting specific requirements.
Inew	Real DC charge-/ discharge current [A].
Pbacnew	Battery power calculated with the new set charge-/ discharge current [A].
SOC	New set SOC value

The AC-current value (=Ibac) is set as a possible maximum charge-/ or discharge current for the battery, which is defined in the microgrid control model by the available remaining PV power after supplying the load. This will first be converted to a DC value to use it for calculating the real possible charge-/ discharge current (= I) and the new SOC of the storage system. The control strategy of the model is based on the charging and discharging current of the battery. It should be considered which specific conditions or limitations are the best to charge any battery. Each battery system has unique needs in terms of charging speed, DOD, loading and exposure to adverse temperature [53]. There are similarities within the battery families, by keeping in mind that these requirements extend to almost all batteries in use. Table 3.3 addresses the limitations of the used battery control model.

Table 3.3 Defined limitations for the battery control model

Limitation	Set new current value [A]
SOC > 0.9 && I>0	Inew = 0
SOC <= 0.2 && I<0	Inew = 0
Tamb <=10 && I>0	Inew = min(Inew, 0.3 * Imax)
Tamb >=30 && I>0	Inew = min(Inew, 0.5 * Imax)
I<0	Inew = max(Inew, -Imax)
I>0	Inew = max(Inew, Imax)

It is defined that the battery should stop charging or discharging if the maximum or minimum state of the charge of the battery is reached. Charging a battery more often is better than draining a battery full, therefore the minimum SOC is set to 20% [29] and maximum SOC to 90% to avoid overcharging the battery. The charging current was limited at different ambient temperatures, which are appointed due to given specification and available operating temperatures in the datasheet. After setting the new charging current due to given parameters, the input SOC and the new current value will be passed to the battery model, where the new SOC is calculated and returned. Finally, the new AC current, the DC current, the output power and the new SOC of the battery are returned to the microgrid model, which will be returned then further for the control purposes to the microgrid control model and saved there for control purposes. The Matlab code structure of the battery control model is attached in Appendix 8.

3.2 Description of flywheel control model

The described simplified flywheel model in chapter 2.2.3 is controlled in two different ways, which will be outlined in subsequent paragraphs.

3.2.1 Moving average control

The moving average control of the flywheel system was used to verify the flywheel system of a previous student work in Matlab m.file [49]. The inputs and outputs of the flywheel control model are listed in Table 3.4 and Table 3.5.

Table 3.4 Flywheel control model inputs

Model inputs	Definition
Model	Selected flywheel type/model
S	historical values of the load profile [kW]
SOC	Initial SOC of the flywheel
Ploadnow	Current power consumption [kW]

Table 3.5 Flywheel control model outputs

Model outputs	Definition
Mov	Moving average value
Ef	Output energy of flywheel [kWh]
Pf	Output power of flywheel [kW]
SOCnew	New determined SOC of flywheel
wnew	New determined angular velocity of flywheel [rad/s]

The length of the moving average value is the input length of the historical values of the load profile, which includes also the current load profile value. The moving average value is calculated by dividing the sum of the historical values by the length of them (Formula (3.1)). Thus, the output power of the flywheel results by subtracting moving average value from the measured power draw of the load. The output energy of flywheel (= Ef) will be calculated then simply by multiplying the output power with 60. This value will be passed then as an input to the flywheel model.

$$Mov = \frac{P}{N} \tag{3.1}$$

where Mov – Moving average value, W

P – sum of the historical load profile values, including the current load, W

N – length of input S

If the returned SOC value from the flywheel model is less than 0.01, the output parameters will be set as follows to avoid negative values of the SOC:

$$Mov = Ploadnow;$$
$$Pf = 0;$$
$$Ef = 0;$$
$$SOCnew = SOC;$$
$$w_{new} = w;$$

That means, that the flywheel will neither be charged nor discharged. The output power and energy of the flywheel is set to zero, the SOC value will stay the same as well as the angular velocity of the flywheel. If the SOC of the flywheel is exceeding the maximum charge capacity (= SOC=1) during charging, the values will be set the same way as mentioned above. This system is quite simple

because is just doing moving average without considering the supplied PV power or charging the flywheel storage system (see Appendix 9). Therefore, a custom control model of the flywheel system was developed to be able to control the microgrid more effectively. In the next chapter the developed custom control model of the flywheel will be explained.

3.2.2 Custom control

The custom control of the flywheel storage system was controlled in different ways. As well as the flywheel MA control the custom control is based on the components PV, load, battery and flywheel storage. The difference to the MA and custom control is that the charge and discharge of the flywheel storage are depending on the generated PV power and load profile. The different algorithms, which were derived, will be explained below.

Algorithm 1

The algorithm 1 aligns the charging and discharging of the flywheel storage system with the PV and load trend. The trend line of PV and load profile is calculated as its slope (=mpv and mload). If the trend line of the generated PV power is positive or greater than the trend line of the load, the flywheel storage will be charged with the available PV power. Likewise, the flywheel will be discharged if the trend line of the load is greater than that of the generated PV power.

Algorithm 2

Algorithm 2 is based on the average historical values of PV and Load profile data (=mpvavg and mloadavg). If the calculated average value of the PV is higher than the calculated average value of the load profile, the flywheel will be charged with the available PV power. Vice versa the flywheel will be discharged with the remaining load power after subtracting the available PV power from the load.

Algorithm 3

This algorithm adjusts the flywheel on the exact PV and load values. The current PV value will be subtracted from the current load value, which results the remaining power 'P_temponew'. If P_temponew is greater than zero, the flywheel will be discharged by this power. That means, that

the power consumption of the load is higher than the generated PV power. In case that P_temponew is smaller than zero the flywheel will be charged by the available PV power.

Algorithm 4

The last algorithm is controlling the flywheel by the predefined time of day. For the control the time between approximately 8am and 7pm were chosen, where is known that at this time PV power should be available. The control algorithm is defined as follows: if during this time the generated PV power is lower than the power consumption the flywheel will be discharged and charged if the power consumption is lower than the generated PV power.

Above, the different control algorithm for defining the flywheel power were explained. The defined flywheel power will be passed further to the object model 'Microgrid_model.m', where the remaining power after PV, load and flywheel will be calculated, which will be the base to decide if the battery storage should be charged or discharged. An overview of the explained control algorithms is given in Table 3.6. The Matlab code of the flywheel custom control model is attached in Appendix 10.

Table 3.6 Overview of used control algorithms

Algorithm	Description of the algorithm
1	Charge flywheel: mpv > mload Discharge flywheel: mpv < mload
2	Charge flywheel: mpvavg > mloadavg Discharge flywheel: mpvavg < mloadavg
3	Charge flywheel: P_temponew < 0 Discharge flywheel: P_temponew > 0
4	Charge flywheel: timestep > 465 && timestep < 1125 && Ppvnew > Ploadnew Discharge flywheel: timestep > 465 && timestep < 1125 && Ppvnew < Ploadnew

4 Matlab simulation of control strategies and test scenarios

The ways how to control the behaviour of the battery and flywheel storage system were discussed in the previous chapters. They are implemented in a separate Matlab file, which just needs the scenario and algorithm number as inputs. The 3 scenarios were categorized into three, defined by switching on or off a certain flywheel control model with the specific control algorithm. The scenario numbers are used to identify the correct scenario in the Matlab code. The first digit represents the battery model type for certain application, the second digit the control scenario and the third digit, if scenario 3 is chosen the algorithm type of the third scenario. An overview on the scenarios with the respective scenario numbers is shown in Table 4.1:

Table 4.1 Scenarios for simulation

Scenario Number	Activated appliances	Control models
1	Battery	Only battery control
2	Battery Flywheel	Battery control Flywheel MA control
3	Battery Flywheel	Battery control Flywheel custom control

All scenarios were conducted for a detached house and settlement microgrid system. Also, an apartment building application is defined in Matlab, due to time constraints it was not presented in this work but can be implemented and analysed easily in future. In the same way another application can be implemented because the framework is already created for different applications. The results of the different scenarios will later be compared regarding their charge cycles, off grid-mode time and cycle lifetime.

Initial parameters and values of the scenarios were chosen as follows:

- The off-grid system has only the PV-system as distributed energy resource
- All necessary variables were initialised and set to one, zero or a more appropriate initial value, like 1 (=full charged) for the initial SOC value of battery and flywheel, 40 °C for the initial ambient temperature, which will be changed in very time step
- Depending on the model number, the corresponding battery, flywheel, PV and load profile types are selected, like:
    - 1 = detached house

    - 2 = apartment building
    - 3 = settlement
    - 4 = general (empty file to be able to integrate a new application)
- All components were deactivated or activated according to the chosen scenario
- The simulation was conducted for 1 day (24 hours)
- For initial examination PV values in September were used, in future different seasons can be analysed
- It is assumed that the PV system includes an inverter, which keeps the system voltage constant
- As a timestep dt=1/60 [h] (= 1 min) was chosen. With 1 min data it could provide more precise results than hourly values. Moreover, the measurement data of PV and Load profile were measured in 1 min time steps

<u>After simulation:</u>

- After the simulations all important output variables and arrays are saved
- The most interesting values, will be plotted then as graphs
- The working principle of the whole simulation and the structure of the complete Matlab code is shown in Figure 2.13, Chapter 2.3 and Appendix 7

The results of the simulated scenarios will be outlined in the next few chapters. Only the results of detached house model are described in detail. However, the results of the model settlement can be seen in the appendix, these will be pointed out in the text.

4.1 Scenario 1: PV with battery storage system

As stated in the heading, the first scenario is just considering the PV and the battery storage system. This is the base scenario and will show, how the battery storage behaves, if it is only working with the existing PV system. The operating principle of the battery control was already explained in chapter 3.1, as well as the measurement data's of the PV system in chapter 2.2.2 and load profile in chapter 2.2.1. After simulation the first scenario, the AC charging/ discharging current of the battery storage is displayed as follows below (see Figure 4.1). As the below graphic shows the battery behaviour works successfully and adequate. The functionality of the battery control system can be seen from the maximum discharge value in the graph with -16.65 A in AC which represents a maximum DC value of -75 A, as previously defined.

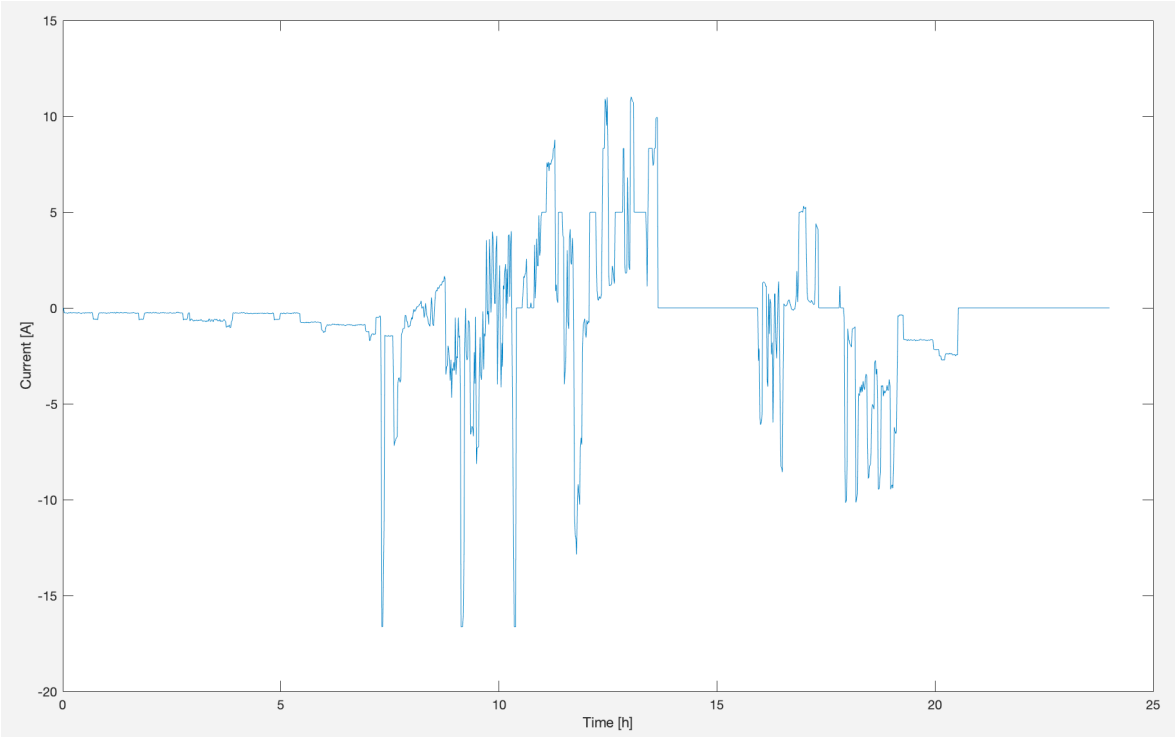

Figure 4.1 Scenario 1: Detached house battery AC charging / discharging current

Also, the SOC simulation confirms the functionality of the battery control system, where the SOC value reaches the upper limit with 90% at maximum PV power generation and lower limit at 20% if the maximum DOD of 80% is reached (see Figure 4.2). In order to make a qualitative statement about the battery system, the battery charging cycles should be analysed. The charge cycles of the battery can be found through the saved values of the SOC simulation. Thereby, the SOC value of the current time step will be subtracted from the SOC value of the previous time step over the

whole operating time. The calculated SOC difference (= SOCdiff) can be negative due to charging or positive due to discharging the battery storage system. All resulting positive values of the SOC values were summed. The same procedure is applied for negative values of the SOC. The sum of all calculated positive SOCdiff gives 108.47% within 24h and 188.69% for the sum of negative SOCdiff. Both these values will be added and dived by two. It follows that the battery is doing 1.4858 cycles in one day. A completely charge and discharge on rechargeable battery is defined as charge cycle. If the charge cycles are extrapolated to one year, it will be reached 542 cycles per year.

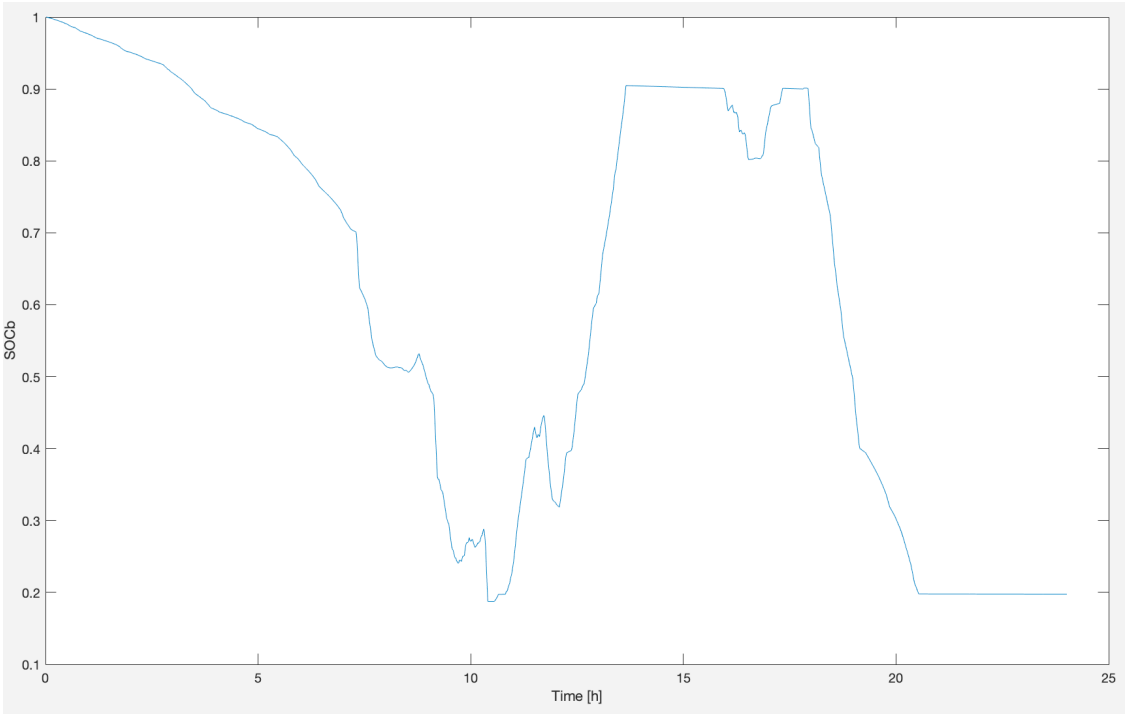

Figure 4.2 Scenario 1: Detached house battery SOC behaviour

The off-grid mode time of scenario 1 is reaching 10h 22min. This value can be detected in Figure 4.3, before a voltage drop is occurring. The reason for the high voltages in the simulation is the generated PV power, which is exceeding. As already mentioned, it is assumed that the PV system includes an inverter, which is controlling the exceeding voltage and keeps the voltage constant at 230 V mains voltage.

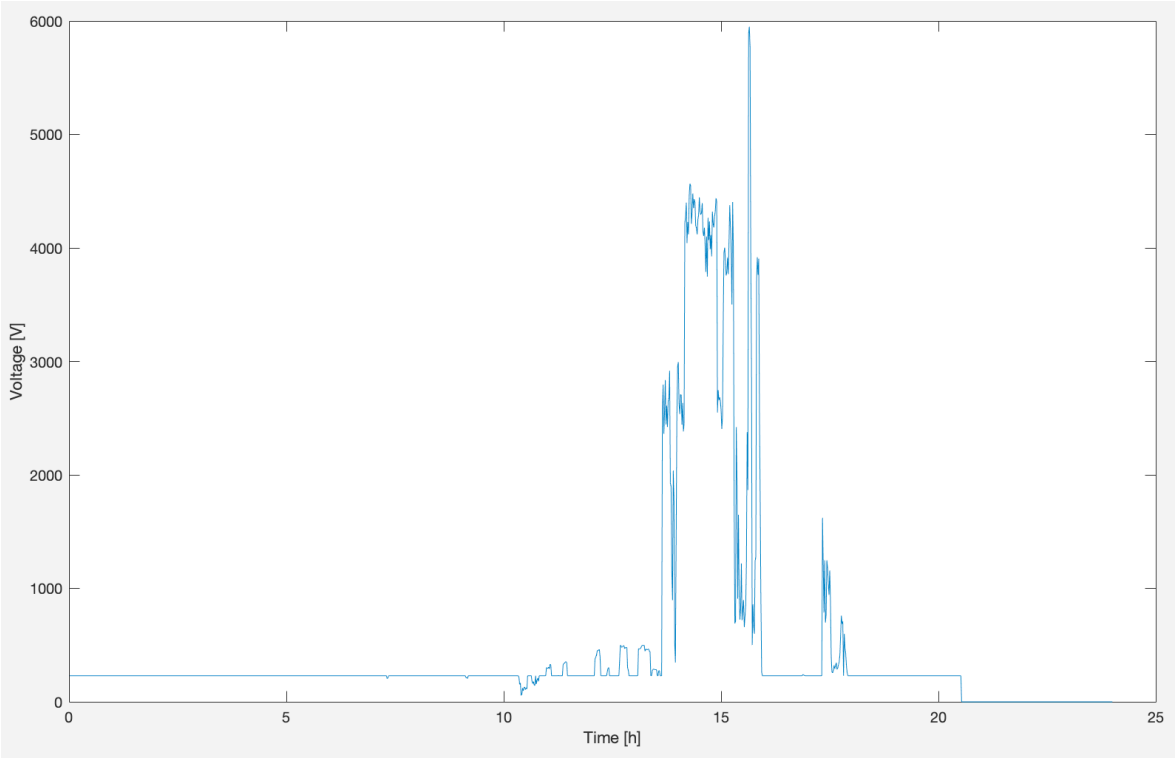

Figure 4.3 Scenario 1: Detached house microgrid system output voltage

The graphs for a settlement simulation are attached in Appendix 11, Appendix 12 and Appendix 13. In Table 4.2 an overview about the settlement simulation results is given.

Table 4.2 Scenario 1: Summary of results

	Detached house	Settlement
SOCdiff charge	108.47%	70.38 %
SOCdiff discharge	188.69%	150.84 %
Charge cycles per day	1,4858 cycle	1.1061 cycle
Charge cycles per year	542 cycles	403 cycles
Max. off-grid time	10h 22min	20h 58min

4.2 Scenario 2: PV with battery and flywheel MA control

The second scenario was done with the battery and flywheel MA control model. Figure 4.4 exposes the AC charging/ discharging current of the battery storage. Comparing Figure 4.4 and Figure 4.1 from scenario 1, there is a difference in the charging and discharging behaviour of the current, which has also an impact on the SOC behaviour of the battery storage. The charging process in Figure 4.4 is done in small steps, as can be seen in more detailed in the figure. A closer look reveals that with the flywheel MA control the battery is discharging less than in scenario 1 without the flywheel. In scenario 1 the discharge current exceeded 16 A, but in the scenario 2, it is now below this value.

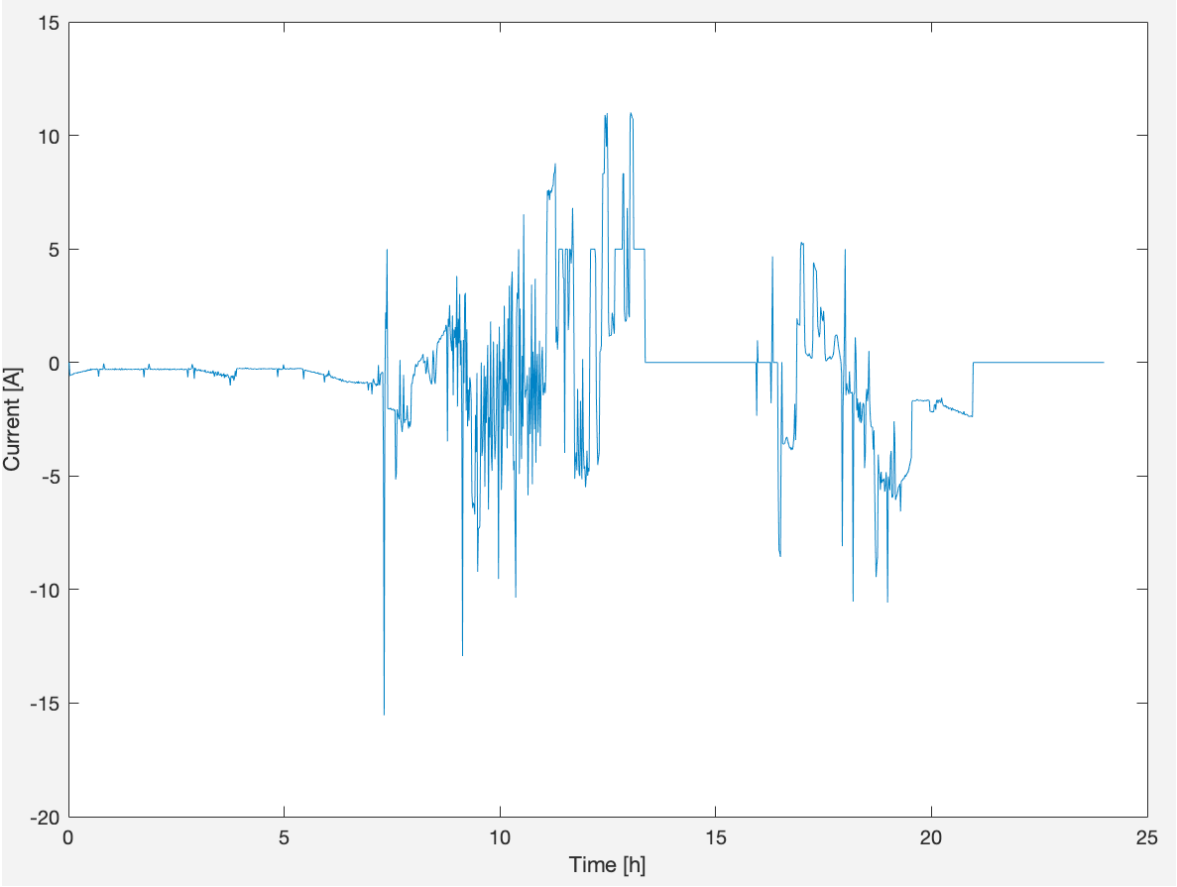

Figure 4.4 Scenario 2: Detached house battery AC charging / discharging current

Due to using the flywheel in this scenario the SOC simulation of the flywheel storage system is also shown (see Figure 4.5). The typical energy storage time of flywheel storage devices is only in the region of 8 to 30 seconds, which makes one of the biggest differences between flywheel storage

devices and batteries [50]. This is also recognisable in their SOC with their fast charging and discharging behaviour.

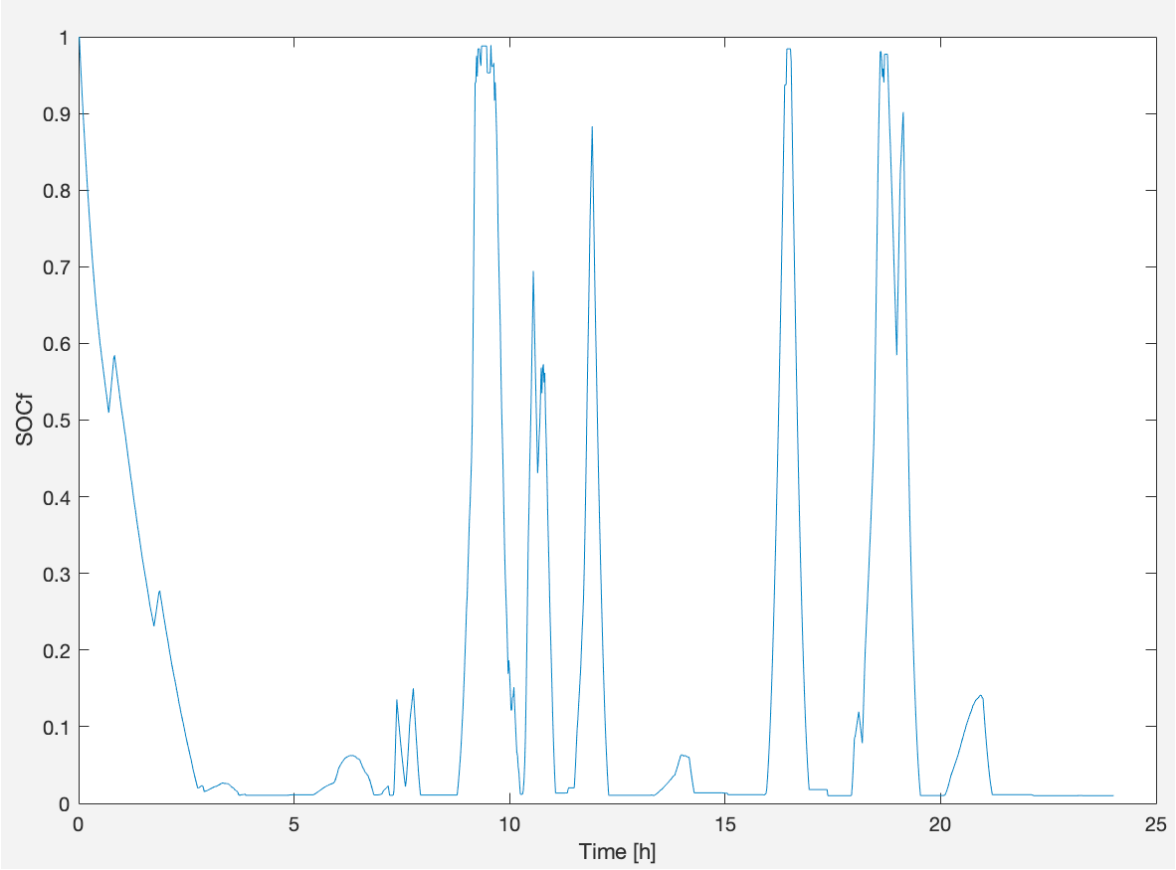

Figure 4.5 Scenario 2: Detached house flywheel SOC behaviour

To be able to compare the difference between scenario 1 and 2 the charge cycle of the battery system was identified. Thus, it could be determined, how much load levelling the modelled flywheel MA control model is doing. It should be considered that this performance is depending on the chosen moving average value of the flywheel MA control model. The operating principle of the flywheel MA control was already explained in chapter 3.2.1. In the following two examples with different MA values will be shown to able to see the changes. The first examples are done with a moving average value of 30, and MA 60, including the current load. This both values were chosen based on previous work, where both values were considered [46]. The identification of the battery charge cycles was done as in the previous chapter for scenario 1. The results of both examples are listed in Table 4.3.

Table 4.3 Scenario 2: Detached house summary results

Detached house	MA: 30	MA:60
SOCdiff charge within 24h	95.73%	84.66%
SOCdiff discharge within 24h	176.07%	165.04%
Charge cycles per day	1.359 cycles	1.2485 cycles
Charge cycles per year	496 cycles	455 cycles
Max. off-grid time	20h 48min	20h 55min

As it can be seen there is a significant difference in charge cycles per year. The battery charge cycle is reduced up to 41 cycles by using MA 60. If they are compared with scenario 1, the charge cycle with MA 30 is reduced by 46 cycles and with MA 60 by 87 cycles. As well as a serious improvement of the off-grid mode time can be observed by comparing the results of scenario 1 detached house in Table 4.2 and Table 4.3. In scenario 1 without flywheel MA control the off-grid mode time was 10h 22min. With the flywheel MA control, the off-grid mode time was increased by 10h. by comparing both figures Figure 4.3 and Figure 4.6 It can be seen that the voltage drop is removed by using the flywheel system.

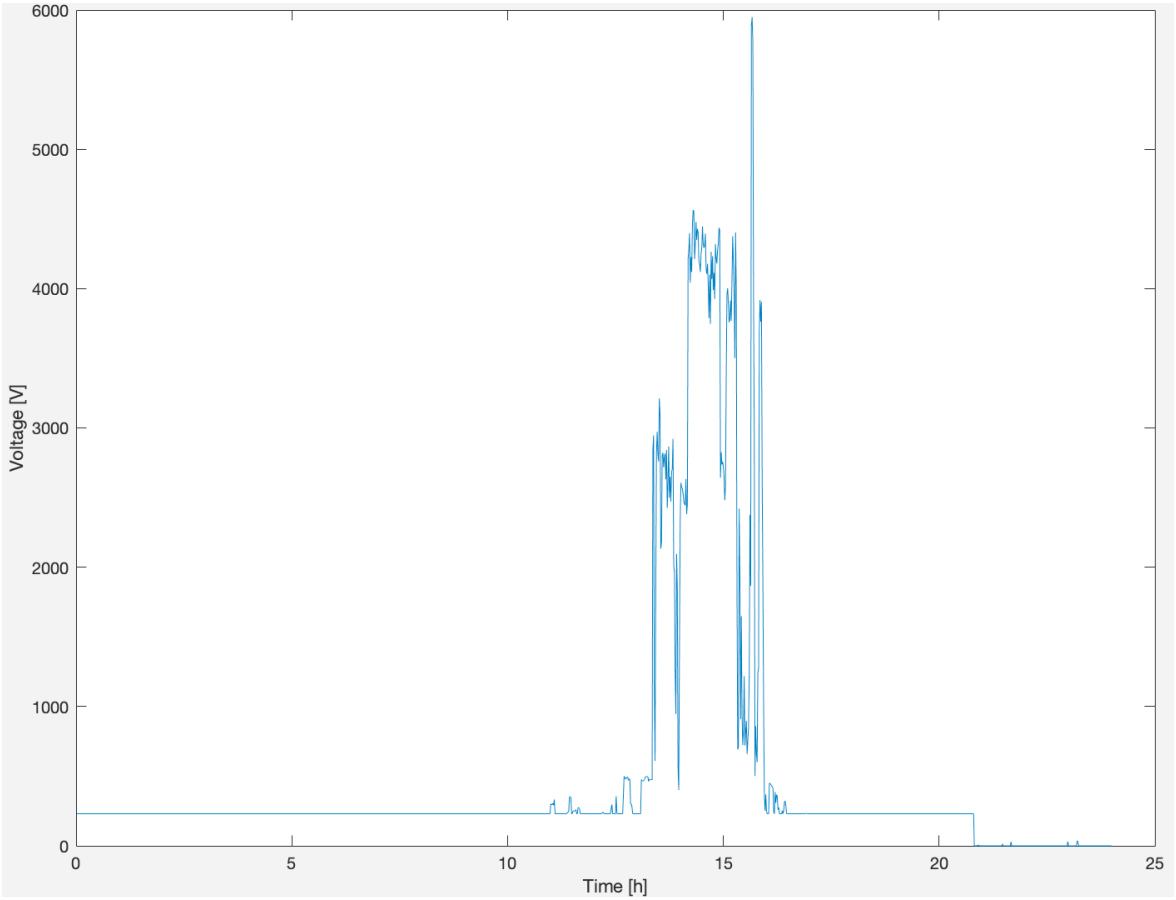

Figure 4.6 Scenario 2: Detached house microgrid system output voltage

Above the simulation results of the scenario 2 with a detached house was shown. The graphical simulation of the settlement can be found in Appendix 14 – 17. The most important values of the settlement simulation, with different MA examples are listed in Table 4.4. Comparing Table 4.4 with Table 4.2, there could not be achieved any improvement with scenario 2, it just remained the same as in scenario 1. The reason for that could be the chosen battery capacity, which is quite enough for a settlement. Different size of batteries and flywheels were not simulated in this work due to limited time frame but should be considered in future, to be able to make better statements about its influence.

Table 4.4 Scenario 2: Settlement summary of results

Settlement results	MA: 30	MA: 60
SOCdiff charge within 24h	70.41%	70.30%
SOCdiff discharge within 24h	150.56%	150.65%
Charge cycles per day	1.105 cycles	1.105 cycles
Charge cycles per year	403 cycles	403 cycles
Max. off-grid time	21h 12min	20h 58min

4.3 Scenario 3: PV with battery and flywheel custom control

The different control algorithms of the flywheel custom control were already explained in Chapter 3.2.2. In the following, the achieved results of the detached house and settlement simulations are shown in Table 4.5 and Table 4.6.

Table 4.5 Scenario 3: Detached house summary results

Algorithm	SOCdiff charge [%]	SOCdiff Discharge [%]	Charge cycles per day	Charge cycles per year	Max. off-grid time
1	63.49	143.67	1.0358	378	21h 06min
2	79.81	159.84	1.1983	437	21h 21min
3	68.82	148.90	1.0886	397	21h 25min
4	58.60	138.63	0.9862	360	21h 22min

As it is shown in Table 4.5 best results for detached house simulation were achieved with algorithm number 1 and 4. The first algorithm has 378 calculated charge cycles and is reaching a maximum

off grid time of 21 hours. By using the fourth algorithm the charge cycles could be decreased to 360 charge cycles per year and the off-grid time could be increased for another half an hour. As well as for the settlement simulation the best results were achieved with these two algorithms, which can be seen in Table 4.6.

Table 4.6 Scenario 3: Settlement summary results

Algorithm	SOCdiff charge [%]	SOCdiff Discharge [%]	Charge cycles per day	Charge cycles per year	Max. off-grid time
1	64.61	144.66	1.0464	382	21h 25min
2	67.92	148.08	1.08	394	21h 07min
3	65.99	146.04	1.0602	387	21h 07min
4	65.18	145.22	1.052	384	21h 07min

4.4 Summary of scenario results

In the previous chapters the simulated scenarios and the different control algorithms of this work were described. The results of all scenarios and control algorithms with the best results are summarised in Table 4.7. In the first column the scenario number is listed. The second column contains the application model, where the abbreviation D stands for ‘detached house’ and S for ‘settlement’. In addition, the cycle lifetime of the battery was calculated. This is resulting by dividing the maximum cycles of battery life, which was taken from the data sheet of the used battery storage system from manufacturer KOKAM with 4500 cycles, by the calculated charge cycles per year [40]. Thus, the cycle lifetime for different scenarios could be achieved in column five. These values are just theoretical values, which based on the given values in the data sheet. To be able to verify these values the proposed control strategies of energy storages should be practically tested. Based on theoretical simulations the cycle lifetime as well as the obtained maximum off-grid time could be increased. The reduction of charge cycles between Scenario 1 and 2 for detached house is 16% by considering the MA 60. Between scenario 1 and 3 the charge cycles could be reduced by up to 34%.

Table 4.7 Scenario results overview

Scenario	Model	Algorithm	Charge cycles/ year	Cycle lifetime [year]	Max. off-grid time
1	D	-	542	8,3	10h 22min
	S	-	403	11	20h 58min
2	D	MA 30	496	9	20h 48min
		MA 60	455	9,9	20h 55min
	S	MA 30	403	11	21h 12min
		MA 60	403	11	20h 58min
3	D	1	378	11,9	21h 06min
		4	360	12,5	21h 22min
	S	1	382	11,7	21h 25min
		4	384	11,7	21h 07min

5 Financial analysis

An important aspect that needs to be considered along with the development is the financing of the project. The financial analysis is based on a grid connected system. It is assumed the same control is used in the islanded system is also used in grid connected mode as it results in a maximum self-consumption control strategy in this case. The benefits of the extended off-grid time, namely potential profit losses due to blackout etc. was not accounted for. The Figure 5.1 describes the financial considerations keeping in mind the payback period.

	PV and battery storage		
	self-financing	**50% loan financing**	**100% loan financing**
Battery storage	5.000 €	5.000 €	5.000 €
Flywheel storage	0 €	0 €	0 €
Price of PV Moduls	4.004 €	4.004 €	4.004 €
Inverter costs	1.812 €	1.812 €	1.812 €
Small parts	1.000 €	1.000 €	1.000 €
Costs for installation and commissioning of the system	900 €	900 €	900 €
sum of acquisition costs	**12.715 €**	**12.715 €**	**12.715 €**
lending rates	0 €	93 €	121 €
sum of expenses	**12.715 €**	**12.808 €**	**12.836 €**
Subsidy per year DE	309,32 €	309,32 €	309,32 €
Saving DE	569,40 €	569,40 €	569,40 €
Subsidy per year EE	166,60 €	166,60 €	166,60 €
Saving EE	227,76 €	227,76 €	227,76 €
running costs	127 €	127 €	127 €
sum of annual income DE	752 €	752 €	752 €
sum of annual income EE	267 €	267 €	267 €
payback period DE [years]	**17**	**17**	**17**
payback period EE [years]	**48**	**48**	**48**

Figure 5.1 Financial analysis of detached house microgrid with PV and battery

As shown in Figure 5.1, three different types of financing were considered. The first financing type is self-financing, where no loan is taken. The second amounts to 50 percent and the third to 100 percent financing. The costs of battery and flywheel storage as well as the costs of small parts and for installation and commissioning of the system is based on approximation, as till date companies have not responded to enquires about pricing. The financial analysis of detached house application is first done without flywheel, to be able to compare it to the expenses and payback period between the two countries Germany and Estonia with different energy storages. The PV modules were chosen from [54]. The costs were then summed up, which gives an acquisitions cost of 12.715 €.

The lending rates, which were summarized with the acquisition cost, were defined according to the maximum loan amount calculator of Swedbank [55]. For the loan amount calculator precondition defined as mentioned in Table 5.1. These are the same for the financial analysis with flywheel storage, except the loan amount.

Table 5.1 Loan conditions detached house (PV and battery)

	50% loan financing	100% loan financing
Loan amount [€]	7500	13000
Total monthly income [€]	2000	2000
Loan term [years]	10	10

In order to promote the use of renewable energy sources and make the energy sector more efficient subsidies are paid out. The subsidy rate in Estonia is 0.0537 €/kWh and 0.0997 €/kWh in Germany [56, 57]. To get the amount of subsidy per year the fed energy per day was multiplied by the subsidy rate and extrapolated to one year. In addition, the savings during off-grid time are calculated by multiplying the consumption during off-grid time by the electricity cost of the respective country. The electricity cost in Estonia is quite low with 0.12 €/kWh in comparing to Germany with 0.30 €/kWh. Thus, results that the subsidies and savings in Germany are higher than in Estonia. This causes a lower payback period for Germany, which can be calculated by dividing the sum of expenses with sum of annual income. To be able to evaluate the proposed project the profitability should be known. The profitability index is an appraisal technique applied to potential capital outlays and is a useful tool for ranking projects because it allows you to quantify the amount of value created per unit of investment [58]. This value is calculated by dividing the present value of future cash flows to be generated by a capital project by the initial cost, or initial investment of the project [58]. The calculated profitability index for the following project is 0.11, which is less than 1 and means that it should not be invested in the project as the costs overweigh the benefits.

In the same way, the calculation was carried out with the flywheel storage. It is recognizable from the Figure 5.2 that the payback period for both countries is substantially higher due to the high cost of the flywheel.

	PV , battery and flywheel		
	self-financing	**50% loan financing**	**100% loan financing**
Battery storage	5.000 €	5.000 €	5.000 €
Flywheel storage	15.000 €	15.000 €	15.000 €
Price of PV Moduls	4.004 €	4.004 €	4.004 €
Inverter costs	1.812 €	1.812 €	1.812 €
Small parts	1.000 €	1.000 €	1.000 €
Costs for installation and commissioning of the system	900 €	900 €	900 €
sum of acquisition costs	**27.715 €**	**27.715 €**	**27.715 €**
lending rates	0 €	131 €	261 €
sum of expenses	**27.715 €**	**27.846 €**	**27.976 €**
Subsidy per year DE	309,32 €	309,32 €	309,32 €
Saving DE	569,40 €	569,40 €	569,40 €
Subsidy per year EE	166,60 €	166,60 €	166,60 €
Saving EE	227,76 €	227,76 €	227,76 €
running costs	277 €	277 €	277 €
sum of annual income DE	651 €	651 €	651 €
sum of annual income EE	117 €	117 €	117 €
payback period DE [years]	**43**	**43**	**43**
payback period EE [years]	**236**	**238**	**239**

Figure 5.2 Financial analysis of detached house microgrid with PV, battery and flywheel

The financial analysis of the settlement application can be found in Appendix 18. For the settlement application only the self-financing was considered.

Summary

The aim of this work was to develop control strategies for energy storages in an islanded microgrid. Therefore, simplified mathematical models of battery and flywheel storage system were used. The main task of the thesis was the integration of a flywheel model for short term load levelling to reduce charging cycles for the battery storage for increased battery lifetime and off grid mode time of the system. Furthermore, the financial aspect of the system should be considered.

In the first part of this thesis an overview of different microgrid topologies and different battery types were given. Comparison with other storage systems such as lead-acid, flow battery and fuel cell, Li-Ion battery is the only energy storage technology, which fulfil system requirements regarding calendar and cycle lifetime, efficiency, response time, power and energy density for microgrids and electric vehicles where they have proved to be the most promising option.

The second part of this thesis presented the development process of the used microgrid components. All the models developed in this work such as battery and flywheel storage are described separately. Subsequently, the whole system consisting of all the modelled components is illustrated with all its behaviours. The models were simplified. Instead of modelling the PV system measurement data of an existing system were used. The required load profiles for the simulations were generated in a software system.

The control strategies for both energy storages battery and flywheel were modelled in the third part of the thesis. Flywheel was controlled in two different ways – moving average and custom control. A base scenario was conducted to obtain a basis for comparison with other control strategies. Afterwards the different scenarios with different control algorithms were simulated and results presented. It was possible to reduce the charging cycles by up to 16% between scenarios 1 and 2 and by up to 34% between scenarios 1 and 3. This also increased cycle life and off-grid time.

In the last step, a financial analysis was done, which is an important aspect that needs to be considered along with the development of the project. This financial analysis showed that the payback period for Germany is lower than Estonia due to higher subsidies and savings in Germany. It could be concluded that for both countries and different microgrid application the investment would be not profitable, because the costs overweigh the benefits.

During this work, many simplifications had to be made, so there are many opportunities for future work. The battery and flywheel model can be optimised. Simulations for different seasons, with different and more load profiles as well as with different energy storage sized can be simulated. A Matlab PV model instead of using historical measurement data can be created. Further, the validation of the used model can be done in future. The models developed in this thesis are planned to be used in supervisors PhD work.

KOKKUVÕTE (Summary in Estonian)

Töö eesmärgiks oli väljatöötada energiasalvestite juhtimisstrateegiad saarestunud mikrovõrgu jaoks. Uurimiseks kasutati akupatareid ja hooratas-energiasalvesti lihtsustatud matemaatilisi mudeleid. Lõputöö peamiseks ülesandeks oli hoorattamudeli integreerimine lühiajaliseks koormuse tasandamiseks, et tagada mikrovõrgus pikem aku eluiga ja saartalitluse töötamise aeg. Samuti tuli vaadelda süsteemi tasuvust.

Töö esimeses osas anti ülevaade erinevatest mikrovõrkude topoloogiatest ja erinevat tüüpi akupatareidest. Võrreldes teiste salvestussüsteemidega, näiteks pliiaku, läbivooluaku ja kütuseelemendiga energiasalvesti, on Li-Ion aku ainus energiasalvestustehnoloogia, mis vastab süsteemi nõuetele, arvestades kalendaarset ja tsüklilist eluiga, tõhusust, reageerimisaega, mikrovõrkude hetkvõimsuse ja energiatiheduse kriteeriume.

Töö teises osa tutvustati mikrovõrkude komponentide mudelite väljatöötamise protsessi. Kõiki selles töös välja töötatud mudeleid, nagu aku ja hooratas-energiasalvesti, kirjeldatakse eraldi. Seejärel kirjeldatakse kogu modelleeritud komponentidest koosnevat süsteemi. Mudelid olid lihtsustatud. PV-süsteemi modelleerimise asemel kasutati olemasoleva süsteemi mõõtmisandmeid. Simulatsioonide jaoks vajalikud koormusprofiilid loodi vastava tarkvaraga.

Töö kolmandas osas modelleeriti nii aku kui ka hooratas-energiasalvesti juhtimisstrateegiad. Hooratast juhiti kahel erineval viisil - libisev keskmine ja kohandatud juhtimine. Erinevaid juhtimisstrateegiaid võrreldi väljatöötatud baasstrateegiaga. Seejärel simuleeriti erinevaid juhtimisalgoritmidega stsenaariume ja tutvustati tulemusi. Laadimistsüklit oli võimalik lühendada stsenaariumi 1 ja 2 vahel kuni 16% ja stsenaariumi 1 ja 3 vahel kuni 34%. Seega teatud juhtimisstrateegiaid kasutades oli võimalik suurendada aku tsüklilist eluiga ja mikrovõrgu saartalitluse kestust.

Viimases osas koostati tasuvusanalüüs, millega tuleb selliste projektide väljatöötamise juures arvestada. Koostatud analüüs näitas, et süsteemi tasuvusaeg on kõrgemate subsiidiumide ja maksude tõttu Saksamaal madalam kui Eestis. Võib järeldada, et mõlemas riigis ja erinevates mikrovõrkude rakendustes pole investeering tasuv, kuna kulud ületavad tulu.

Tulevikus on töös kasutatud ja väljatöötatud lihtsustatud mudeleid võimalik oluliselt täiustada. Aku ja hooratta mudelit saab optimeerida. Tulevikus saab süsteemi toimist täiendavalt uurida kasutades eri aastaaegade koormusprofiile, toodangu profile ning erinevaid energiasalvestite suurust. Ajalooliste mõõtmisandmete kasutamise asemel saab luua Matlabi PV-mudeli. Selles lõputöös välja töötatud mudeleid on kavas kasutada ka juhendaja doktoritöös.

References

[1] K. D. Patlitzianas, A. Flamos, H. Doukas, A. G. Kagiannas and J. Psarras, "Renewable Energy Sources," in *2004 New and renewable energy technologies for sustainable development*, Singapore, World Scientific, 2007, p. 1.

[2] G. N. Tiwari and R. K. Mishra, Advanced Renewable Energy Sources, Cambridge: Royal SOCiety of Chemistry, 2012.

[3] Dr. M. Bockhorst, "Energieinfo," [Online]. Available: http://www.energieinfo.de/eglossar/energiekrise.html. [Accessed 27 February 2019].

[4] L. Czarnecki, "Photovoltaik: Grundlagen, Systeme und Betrieb," bookboon, 2018.

[5] S. C. Bhatia, Advanced renewable energy systems, New Delhi: Woodhead Publishing India Pvt. Ltd, 2014.

[6] S. Kalaiselvam and R. Parameshwaran, Thermal Energy Storage Technologies for Sustainability: Systems Design, Assessment and Applications, San Diego: Elsevier Science & Technology, 2014.

[7] Florian, "gridx," [Online]. Available: https://gridx.de/2018/02/08/microgrids-und-die-dezentrale-energiewende/. [Accessed 28 February 2019].

[8] S. Borlase, Smart Grids: Infrastructure, Technology and Solutions, Boca Raton: Taylor & Francis Group, 2013.

[9] D. W. Gao, Energy Storage for Sustainable Microgrid, San Diego: Elsevier Science & Technology, 2015.

[10] F. P. Sioshansi , Smart Grid: Integrating Renewable, Distributed & Efficient Energy, Massachusetts: Elsevier, 2012.

[11] T. Funabashi, Integration of Distributed Energy Resources in Power Systems: Implementation, Operation, and Control, San Diego: Elsevier, 2016.

[12] E. Unamuno and J. A. Barrena, "Hybrid ac/dc microgrids—Part I: Review and classification of topologies," *Renewable and Sustainable Energy Reviews,* vol. 52, p. 1251–1259, December 2015.

[13] "photovoltaik.org," [Online]. Available: https://www.photovoltaik.org/wissen/on-grid-und-off-grid. [Accessed 27 March 2019].

[14] Kansas State University, "K-State Research Exchange," 2013. [Online]. Available: https://krex.k-state.edu/dspace/handle/2097/16823. [Accessed 28 February 2019].

[15] N.W.A. Lidula and A.D. Rajapakse, "Microgrids research: A review of experimental microgrids and test systems," Manitoba, 2010.

[16] A. M. R. Lede, M. G. Molina, M. Martinez, P. E. Mercado, "Microgrid Architectures for Distributed Generation: A Brief Review," in *2017 IEEE PES Innovative Smart Grid Technologies Conference*, Quito, 2017.

[17] M T. Lawder, B. Suthar, P. W. C. Northrop, S. De, C. M. Hoff, O. Leitermann, M. L. Crow, S. Santhanagopalan, and V. R. Subramanian, "Battery Energy Storage System (BESS) and Battery Management System (BMS) for Grid-Scale Applications," *Proceedings of the IEEE,* vol. 102, no. 6, pp. 1014-1030, 2014.

[18] P. Gevorkian, Large-Scale Solar Power Systems - Construction and Economics, New York: Cambridge University Press, 2012.

[19] N. Nitta, F. Wu, J. T. Lee, and G. Yushin, "Li-ion battery materials: Present and future," in *Matetrials Today*, 2015.

[20] P. Nikolaidis, A. Poullikkas, "A comparative review of electrical energy storage systems for better sustainability," *Journal of Power Technologies,* vol. 97, no. 3, pp. 225-226, 2017.

[21] "Battery University," [Online]. Available: https://batteryuniversity.com/learn/article/lead_based_batteries. [Accessed 9 May 2019].

[22] L. Lu and N Hu, Recent Advances in Energy Storage Materials and Devices, Millersville: Materials Research Forum LLC, 2017.

[23] T. Elmern, M. Worall, S. Wu, S. B. Riffat, „Fuel cell technology for domestic built environment applications: State of-the-art review,“ *Renewable and Sustainable Energy Reviews,* Bd. 42, pp. 913-931, 2015.

[24] A. Rahomoun, „Mathematical Modelling and Analysis of a Battery Energy Storage System for Microgrids,“ Ph.D. dissertation, School of Engineering, Tallinn University of Technology, Tallinn, 2017.

[25] "Battery University," [Online]. Available: https://batteryuniversity.com/learn/archive/whats_the_best_battery. [Accessed 9 May 2019].

[26] "Speichermonitoring," [Online]. Available: http://www.speichermonitoring.de/ueber-pv-speicher/batterietechnologien.html. [Accessed 10 May 2019].

[27] "Microgrid Knowledge," [Online]. Available: https://microgridknowledge.com/electric-vehicle-batteries-in-microgrids/. [Accessed 10 May 2019].

[28] "Battery University," [Online]. Available: https://batteryuniversity.com/learn/article/battery_test_methods. [Accessed 10 May 2019].

[29] "Battery University," [Online]. Available: https://batteryuniversity.com/learn/article/how_to_make_batteries_more_reliable_and_longer_lasting_1. [Accessed 13 May 2019].

[30] "Battery University," [Online]. Available: https://batteryuniversity.com/index.php/learn/article/how_to_monitor_a_battery. [Accessed 30 May 2019].

[31] "Battery University," [Online]. Available: https://batteryuniversity.com/learn/article/battery_definitions. [Accessed 30 May 2019].

[32] M T. Lawder, B. Suthar, P. W. C. Northrop, S. De, C. M. Hoff, O. Leitermann, M. L. Crow, S. Santhanagopalan, and V. R. Subramanian, „Battery Energy Storage System (BESS) and Battery Management System (BMS) for Grid-Scale Applications,“ *Proceedings of the IEEE,* Bd. 102, Nr. 6, pp. 1014-1030, 2014.

[33] Z. Miao, L. Xu, L. Fan and V. R. Disfani, „An SOC-Based Battery Management System for Microgrids,“ *IEEE Transactions on Smart Grid,* Bd. 5, Nr. 2, pp. 966-973, 2013.

[34] I. D. Serna-Suárez, G. Ordóñez-Plata, G. Carrillo-Caicedo, "Microgrid's Energy Management Systems: A survey," in *2015 12th International Conference on the European Energy Market (EEM)*, Lisbon, 2015.

[35] H. Zhou, T. Bhattacharya, D. Tran, T. S. T. Siew and A. M. Khambadkone, "Composite Energy Storage System Involving Battery and Ultracapacitor with Dynamic Energy Management in Microgrid Applications," *IEEE Transactions on power electronics,* vol. 26, no. 3, pp. 923-930, 2011.

[36] B. Amri and Soedibyo, "Design of batteries charging by charge management concepts on photovoltaic standalone system," in *2016 International Seminar on Application for Technology of Information and Communication (ISemantic)*, Semarang, Indonesia, 2016.

[37] A. Rahmoun, H. Biechl and A. Rosin, "Evaluation of Equivalent Circuit Diagrams and Transfer Functions for Modeling of Lithium-Ion Batteries," *Electrical, Control and Communication Engineering,* vol. 2, no. 1, pp. 34-39, 2013.

[38] Maxime Legraive, "Realisation of a Lithium-ion Battery Model for Microgrid Applications and Validation with Real-time Simulation Platform," Dissertation, Electro-mechanical Engineering with Specialization in Energy, Université catholique de Louvain, Ottignies-Louvain-la-Neuve, Belgium, 2017.

[39] Y. Tian, D. Li, J. Tiana, B. Xia, "State of charge estimation of lithium-ion batteries using an optimal adaptive gain nonlinear observer," *Electrochimica Acta,* vol. 225, pp. 225-234, 2017.

[40] "Kokam," [Online]. Available: http://kokam.com/data/KBM255_series_2018.pdf. [Accessed 15 June 2019].

[41] "Kokam," [Online]. Available: http://kokam.com/data/2019_Kokam_ESS_Brochure.pdf. [Accessed 15 June 2019].

[42] Wen-Yeau Chang, "The State of Charge Estimating Methods for Battery: A Review," *ISRN Applied Mathematics,* p. 7, 5 July 2013.

[43] "Battery University," [Online]. Available: https://batteryuniversity.com/learn/article/elevating_self_discharge. [Accessed 25 June 2019].

[44] D. Yan, L. Lu, F. Jiang, M. Ouyang, "Comparing the performances of different energy storage cells for hybrid electric vehicle," in *EVS28 International Electric Vehicle Symposium and Exhibition*, Korea, 2015.

[45] Noah Pflugradt, "Load Profile Generator," 2016. [Online]. Available: https://www.loadprofilegenerator.de. [Accessed 21 10 2019].

[46] PVGIS, "Photovoltaic Geographical Information System," 22 09 2017. [Online]. Available: https://re.jrc.ec.europa.eu/pvg_download/data_download.html. [Accessed 29 10 2019].

[47] PVGIS European Communities, "EU Commission," [Online]. Available: https://re.jrc.ec.europa.eu/pvg_static/methods.html. [Accessed 4 November 2019].

[48] "wegatech," 2019. [Online]. Available: https://www.wegatech.de/ratgeber/photovoltaik/photovoltaikanlagen/. [Accessed 19 10 2019].

[49] F. Plaum, "Development of power conditioning control strategies for flywheel storage in microgrid," Master thesis, School of Engineering, Tallinn University of Technology, Tallinn, 2019.

[50] Dipl.-Ing Frank Herener, Piller Group GmbH, "Batteries and flywheels and their application in UPS systems," 2011. [Online]. Available: http://www.piller.com/en-GB/documents/2133/batteries-and-flywheels-en.pdf. [Accessed 5 November 2019].

[51] "Sandia," [Online]. Available: https://www.sandia.gov/ess-ssl/docs/pr_conferences/2014/Thursday/Session7/02_Areseneaux_Jim_20MW_Flywheel_Energy_Storage_Plant_140918.pdf. [Accessed 20 October 2019].

[52] International Electrotechnical Commission standard IEC 60038, "IEC Standard V oltages," IEC, Geneva, Switzerland, 2009.

[53] "Battery University," [Online]. Available: https://batteryuniversity.com/learn/article/how_to_prolong_lithium_based_batteries. [Accessed 16 November 2019].

[54] Bosswerk GmbH & Co. KG, "Greenakku," 2019. [Online]. Available: https://greenakku.de/Solarmodule/Solarmodule-ab-200Wp/Q-PEAK-DUO-G5-Solarmodul-Monokristallin-330Wp::1907.html. [Accessed 15 November 2019].

[55] Swedbank, "Swedbank," [Online]. Available: https://www.swedbank.ee/private/credit/loans/home?language=ENG. [Accessed 16 November 2019].

[56] Elering AS, "Elering," [Online]. Available: https://elering.ee/en/renewable-energy-subsidy. [Accessed 16 November 2019].

[57] Bundesnetzagentur für Elektrizität, Gas, Telekommunikation, Post und Eisenbahnen, "Bundesnetzagentur," 2019. [Online]. Available: https://www.bundesnetzagentur.de/DE/Sachgebiete/ElektrizitaetundGas/Unternehmen_Institutionen/ErneuerbareEnergien/ZahlenDatenInformationen/EEG_Registerdaten/EEG_Registerdaten_node.html;jsessionid=137ADD0E59C454AE900265BB2AB8A10C. [Accessed 16 November 2019].

[58] Rosemary Peavler, "The balance small business," 14 January 2019. [Online]. Available: https://www.thebalancesmb.com/the-profitability-index-392917. [Accessed 16 November 2019].

APPENDICES

Table A1.1 Battery specification numbers

Battery Type for:	Specification Number
Detached_house	1
Apartment building	2
Settlement	3
General	4

Appendix 2 Matlab code for the battery self-discharge

```
function [dSOC]=Battery_selfdischarge(SOC, I, dt, Tamb)

%self-discharge proportion; s = self-discharge in %
%the values of the parameters, are calculated with help of linear
%approximation and interpolation!

k = [11.6 9.3 5.1 2.3];
S = [1 0.6 0.4 0.1];

knew= interp1(S, k, SOC) * (10^-8);

l = [3.3 2.5 1.1 0.6];
lnew = interp1(S,l, SOC)*(10^-5);

m = knew * SOC;
c = lnew * SOC;
s1= Tamb * m + c;      %s1 is describing the self-discharge proportion
                       %depending on the various temperature and SOC!

if I==0;
   s2=(3.472*10^-5);
else
   s2=0;
end

dSOC = -((s1+(s2*SOC) * dt));

end
```

Appendix 3 Matlab code for the capacity retention

```
function [Cmax] = Battery_Tamb(Tamb)

%Input Tamb is used as interpolation points

T = [-20 -10 0 10 20 30 40];
C = [0.5 0.7 0.8 0.9 0.98 1 1]; %available capacity in %

%Interpolation

Cmax= interp1(T, C, Tamb);


%figure ('Name', 'C');
%plot(Tamb, Cnew)
%xlabel('T [∞C]')
%ylabel('C [%]')


end
```

Appendix 4 Matlab code for battery model

```
function [SOC] = Battery_model(model,SOCinit,I,dt,Tamb)
%MODEL_BATTERY
%input parameter 'model' is loading a parameter file of a specific battery

switch model
  case 1
     load ('battery_models/detached_house');
  case 2
     load ('battery_models/apartment_building');
  case 3
     load ('battery_models/settlement');
  case 4
     load ('battery_models/general');
end

%Battery is full charged if SOC=1;
%Battery is empty if SOC=0;
%I = battery charge/discharge current; -I if discharging; +I if charging
%Cbatt = battery actual capacity;
%eff = efficiency;

if I>0
  BT=(eff*(I/(Cbatt*Battery_Tamb(Tamb))))*dt;
else
  BT=((1/eff)*(I/(Cbatt*Battery_Tamb(Tamb))))*dt;
end

SOC = (SOCinit + BT + Battery_selfdischarge(SOCinit,I,dt, Tamb));

end
```

Appendix 5 Scaling existing PV system for settlement

Table A5.1 Scaling factor determination of settlement

Power consumption	197849	kWh/year
Solar electricity generation Estonia	864	kWh/kWp
Minimum required system output	229	kWp
Surcharge for battery losses (25%)	49462	kWh/year
Power consumption + surcharge	247311	kWh/year
New minimum required system output	286	kWp
Required power generation per day	678	kWh
Total power output of existing PV on 24. Sept.	803	kWh
Scaling factor for 24. Sept.	**0.844**	

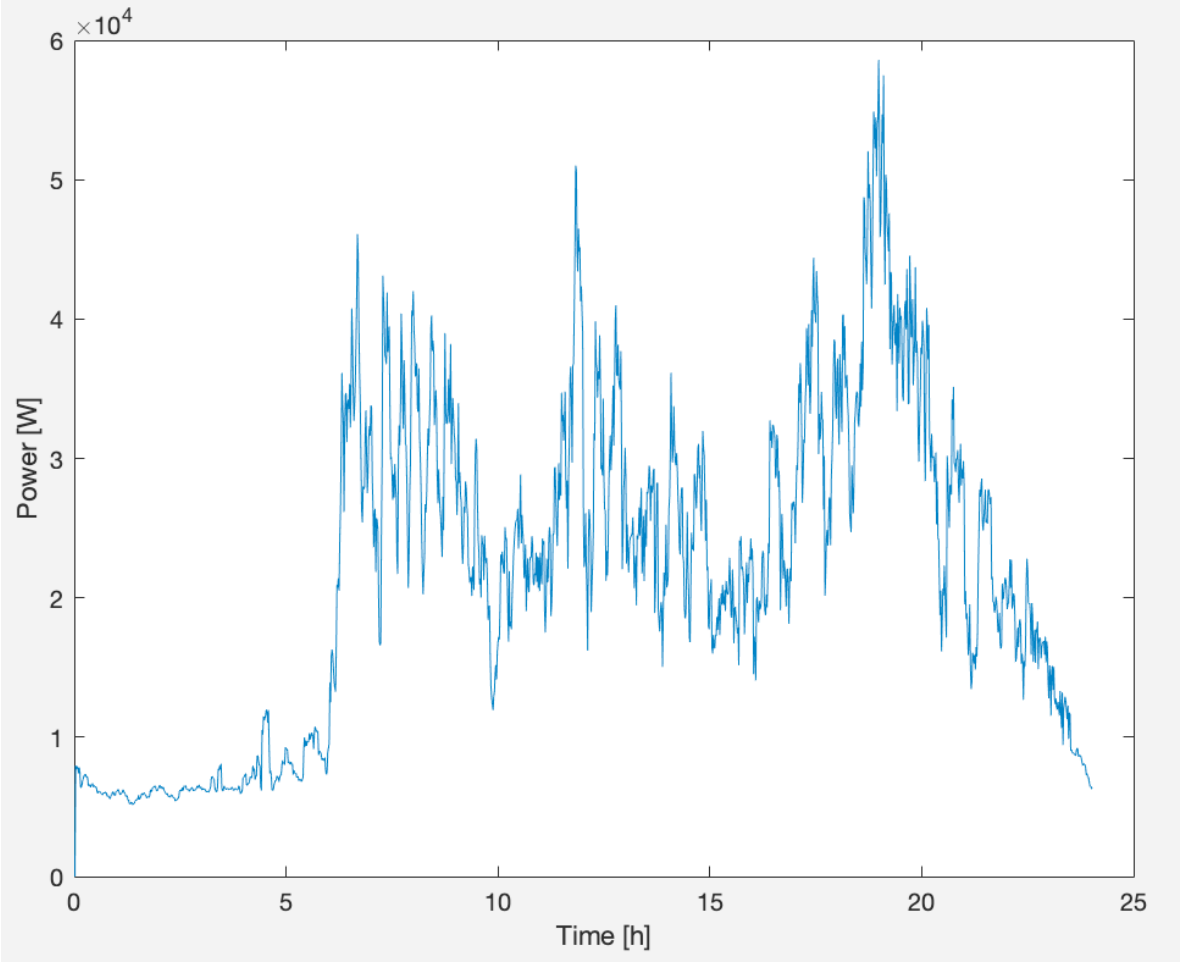

Figure A6.1 Generated load profile of settlement

Table A6.1 Settings overview of settlement

Overview Settlement	
People	Families, Couples, Singles, Student Flattering, Retired Couples
Size	61 households
Power consumption	197 MWh/ year
Measurement data	Per minute
Duration	1 year

```
function [Ppvnew Ipvnew Epvnew Eloadnew Ploadnew Iloadnew P_temponew E_temponew
Pbacnew...
   Ibacnew Ibat SOCbnew Ef Pfnew Ifnew SOCfnew M P_prel I_tot P_tot V_sys wnew mpv mload
Sload]=...
   Microgrid_model(model,SOCb, SOCf, Ibac, dt,Tamb,timestep,Ppv, Iload,P_h, S_h,x, Pf,
If,control)

V_eff=230; %mains voltage                    %[V]
eff_c=0.985; %converter efficiency
%%%%%%%%%%%%%%%%%%%%%%%%%%%%%%%%%%%%%%
%PV Model
Pv=P_h(1428+timestep:1438+timestep,1);
Ppvnew= P_h(1439+timestep,1);          %PV power output    %[W]
Ipvnew=Ppvnew/V_eff;                   %PV cuurent AC      %[A]
Epvnew = (Ppvnew*dt);                  %PV energy          %[Wh]

%%%%%%%%%%%%%%%%%%%%%%%%%%%%%%%%%%%%%%
%Load Profile
Sl=S_h(1428+timestep:1438+timestep,1)./dt;

Sload= S_h(1380+timestep:1439+timestep,1)./dt;   %N=60      %[W]
% Sload= S_h(1400+timestep:1439+timestep,1)./dt;   %N=30      %[W]

Eloadnew= S_h(1439+timestep,1);        %Energy load        %[Wh]
Ploadnew= Eloadnew/dt;                 %Load power         %[W]
Iloadnew= Ploadnew/V_eff;              %Load current AC    %[A]

%Power temporary
P_temponew=Ploadnew-Ppvnew;                          %[W]
E_temponew=P_temponew*dt;                            %[Wh]
%%%%%%%%%%%%%%%%%%%%%%%%%%%%%%%%%%%%%%
%Battery Model
```

```
switch model
  case 1
      load ('battery_models/detached_house');
  case 2
      load ('battery_models/apartment_building');
  case 3
      load ('battery_models/settlement');
  case 4
      load ('battery_models/general');
end

[Ibacnew Pbacnew SOCbnew Ibat]=Battery_control(model,SOCb,Ibac,dt,Tamb);
%%%%%%%%%%%%%%%%%%%%%%%%%%%%%%%%%%%%%%
% Flywheel Model

switch model
   case 1
      load ('Flywheel_Data/Flywheel_data_detached_house.mat');
   case 2
      load('Flywheel_Data/Flywheel_data_apartment_building.mat');
   case 3
      load('Flywheel_Data/Flywheel_data_settlement.mat');
   case 4
      load('Flywheel_Data/Flywheel_data.mat');
end

if x==1 % Flywheel MA control:
   [M Ef Pfnew SOCfnew wnew ]=Flywheel_MA_control(model,Sload, SOCf, Ploadnew);

elseif x==2 %Flywheel custom control:
   [M Ef Pfnew SOCfnew wnew mpv mload]=Flywheel_Custom_control(model,dt, Sl,SOCf,
Ploadnew,...
      Pv, Ppvnew,P_temponew, timestep, control);

else
```

```
    M=0;
    Ef=0;
    Pfnew=0;
    SOCfnew=0;
    wnew=0;
end

Ifnew= Pfnew/V_eff;             %Flywheel current AC [A]
P_prel = Ploadnew+Pfnew-Ppvnew;     %[W]



%%%%%%%%%%%%%%%%%%%%%%%%%%%%%%%%%%%%%%
if x>0
    I_tot=Iload+Ibacnew*(Ibacnew>0)+If*(If>0);
    P_tot=Pbacnew*(-1)*(Pbacnew<0)+Pf*(-1)*(Pf<0)+Ppv;
else
    I_tot = Iload+Ibacnew*(Ibacnew>0);
    P_tot=Pbacnew*(-1)*(Pbacnew<0)+Ppv;

end

 if I_tot ~=0
     V_sys=P_tot/I_tot;
 else
     V_sys = V_eff;
 end

end
```

Appendix 8 Matlab code for battery control

```
Function [Ibacnew,Pbacnew, SOC, Inew] = Battery_control(model,SOC,Ibac,dt,Tamb)
V_eff=230;   %mains voltage
eff_c=0.985; %converter efficiency

switch model
  case 1
     load ('battery_models/detached_house');
  case 2
     load ('battery_models/apartment_building');
  case 3
     load ('battery_models/settlement');
  case 4
     load ('battery_models/general');
end

I=(Ibac*V_eff)/(eff_c*Vnom);
Inew=I;

if SOC>0.9 && I>0
   Inew=0;
elseif SOC<=0.2 && I<0
   Inew=0;
end


if Tamb <=10 && I>0
   Inew=min(Inew,0.3*Imax);
elseif Tamb >=30 && I>0
   Inew=min(Inew,0.5*Imax);
end


if I<0
```

```
    Inew=max(Inew,(-Imax));
elseif I>0
    Inew=min(Inew, Imax);
end


SOC = Battery_model(model,SOC,Inew,dt,Tamb);

Pb=Vnom*Inew;
Pbacnew=Pb*eff_c;
Ibacnew=Pbacnew/V_eff;

end
```

Appendix 9 Matlab code for flywheel MA control

```
function[Mov, Ef, Pf, SOCnew, wnew]= Flywheel_MA_control(model,S, SOC, Ploadnow)

switch model
   case 1
      load ('Flywheel_Data/Flywheel_data_detached_house.mat');
   case 2
      load('Flywheel_Data/Flywheel_data_apartment_building.mat');
   case 3
      load('Flywheel_Data/Flywheel_data_settlement.mat');
   case 4
      load('Flywheel_Data/Flywheel_data.mat');
end


dt = 1/60;                  %[h]->1min
N=length(S);                %N= Amount of Moving average values
P=sum(S);                   %Power [W]

%M is Moving average value from the measured power draw of the load:
Mov = (P/N);                %Moving average value [W]

%Pf is power output of flywheel, calculated by subtracting
%the Moving average value from the measured power draw of the load
Pf=(S(N)-Mov);              %Power output flywheel [W]
Ef=Pf*dt;                   %Energy flywheel [Wh]


[SOCnew, w, wnew]=Flywheel_model(model,SOC,Ef);



if  SOCnew < 0.01
```

```
    Mov = Ploadnow;
    Pf = 0;
    Ef = 0;
    SOCnew = SOC;
    wnew = w;
elseif SOCnew >0.99
    Pf = 0;
    Ef = 0;
    SOCnew = SOC;
    wnew = w;
end

Pf=Pf*(-1);
% SOCnew=1;

end
```

Appendix 10 Matlab code for flywheel custom control

```
function[M, Ef, Pf, SOCnew, wnew, mpvavg, mloadavg]= Flywheel_Custom_control(model,dt,
S,SOCf, Ploadnew,...
   Pv, Ppvnew, P_temponew, timestep, control)

switch model
   case 1
      load ('Flywheel_Data/Flywheel_data_detached_house.mat');
   case 2
      load('Flywheel_Data/Flywheel_data_apartment_building.mat');
   case 3
      load('Flywheel_Data/Flywheel_data_settlement.mat');
   case 4
      load('Flywheel_Data/Flywheel_data.mat');
end
M=0;
V_eff=230;

N=length(Pv);
L=length(S);

mpv= (Pv(N)-Pv(1))/(N-1); %slope of pv
mload= (S(L)-S(1))/(L-1); %slope of load
mpvavg=sum(Pv)/N;
mloadavg=sum(S)/L;


switch control
   case 1
      if  mpv>mload
         Pf=0;
         Premain=abs(Ppvnew);
         Ef=Premain*dt;
      elseif mpv<mload
```

```
        Premain=abs(Ppvnew-Ploadnew);
        Pf=Premain*(-1);
        Ef=Pf*dt;
    end

case 2
    if mpvavg > mloadavg
        Pf=0;
        Premain=abs(Ppvnew);
        Ef=Premain*dt;
    elseif  mpvavg < mloadavg
        Premain=abs(Ppvnew-Ploadnew);
        Pf=Premain*(-1);
        Ef=Pf*dt;
    end


case 3
    if P_temponew > 0
        Premain=abs(Ppvnew-Ploadnew);
        Pf=Premain*(-1);
        Ef=Pf*dt;
    else
        Pf=0;
        Premain=abs(Ppvnew);
        Ef=Premain*dt;
    end


case 4
    if timestep>465 && timestep<1125 && Ppvnew<Ploadnew
        Premain=abs(Ppvnew-Ploadnew);
        Pf=Premain*(-1);
        Ef=Pf*dt;
    else timestep>465 && timestep<1125 && Ppvnew>Ploadnew
```

```
        Pf=0;
        Premain=abs(Ppvnew);
        Ef=Premain*dt;
    end
end


[SOCnew, w, wnew]=Flywheel_model(model,SOCf,Ef);


if  SOCnew < 0.01
   Pf = 0;
   Ef = 0;
   SOCnew = SOCf;
   wnew = w;
elseif SOCnew >0.99
   Pf = 0;
   Ef = 0;
   SOCnew = SOCf;
   wnew = w;
end


end
```

Appendix 11 Scenario 1: Settlement battery AC charging / discharging current

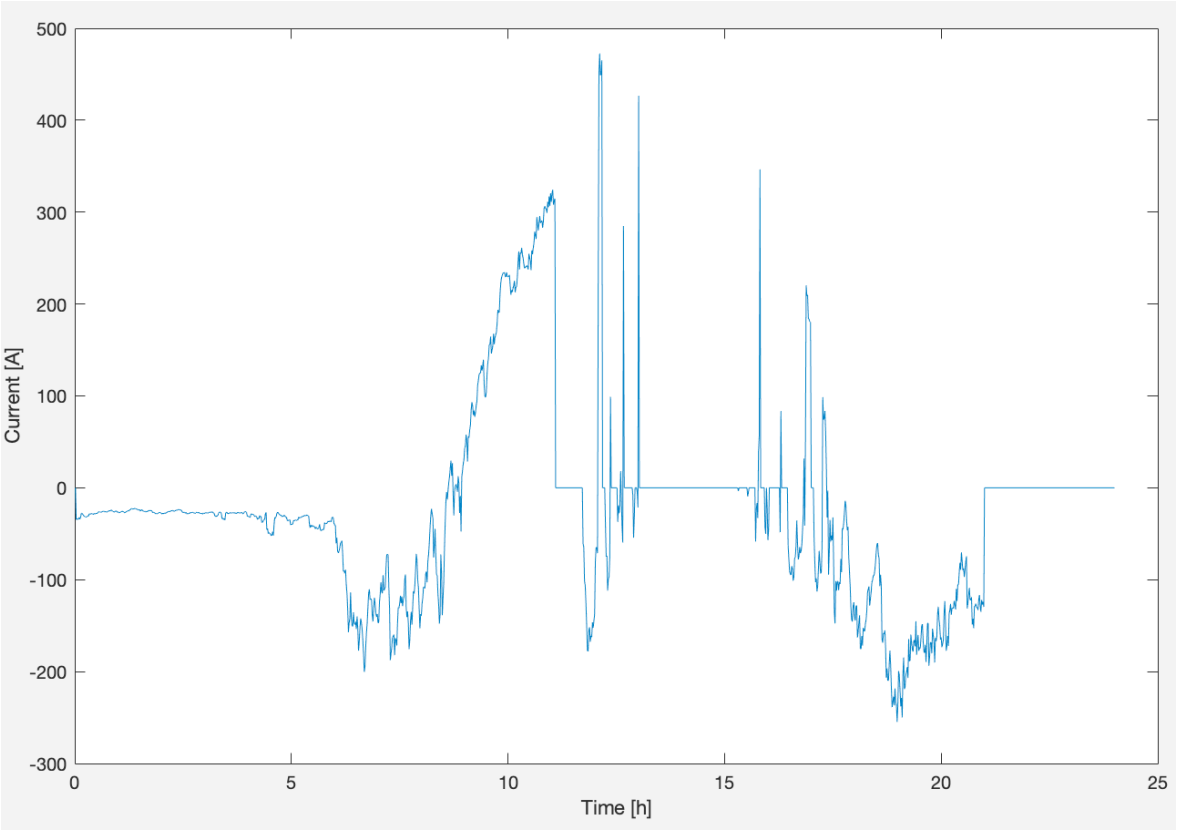

Figure A11.1 Scenario 1: Settlement battery AC charging / discharging current

Appendix 12 Scenario 1: Settlement battery SOC behaviour

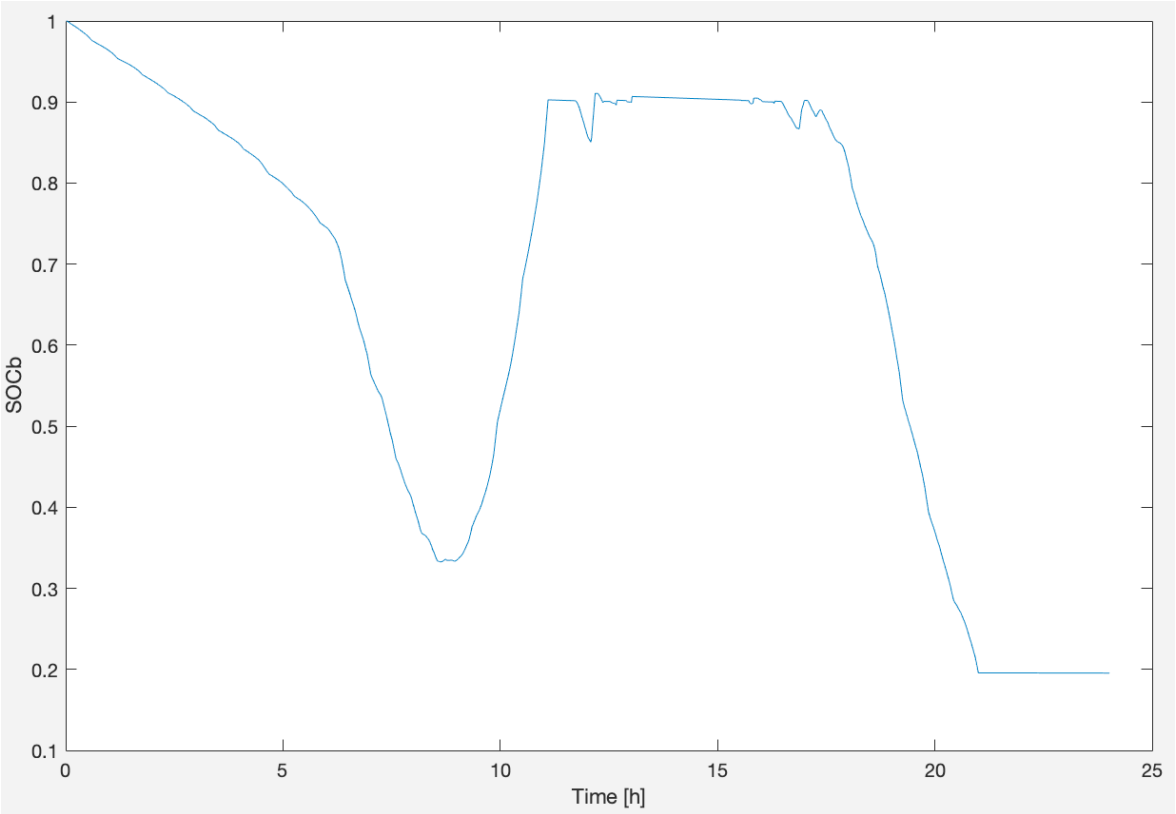

Figure A12.1 Scenario 1: Settlement battery SOC behaviour

Appendix 13 Scenario 1: Settlement microgrid system output voltage

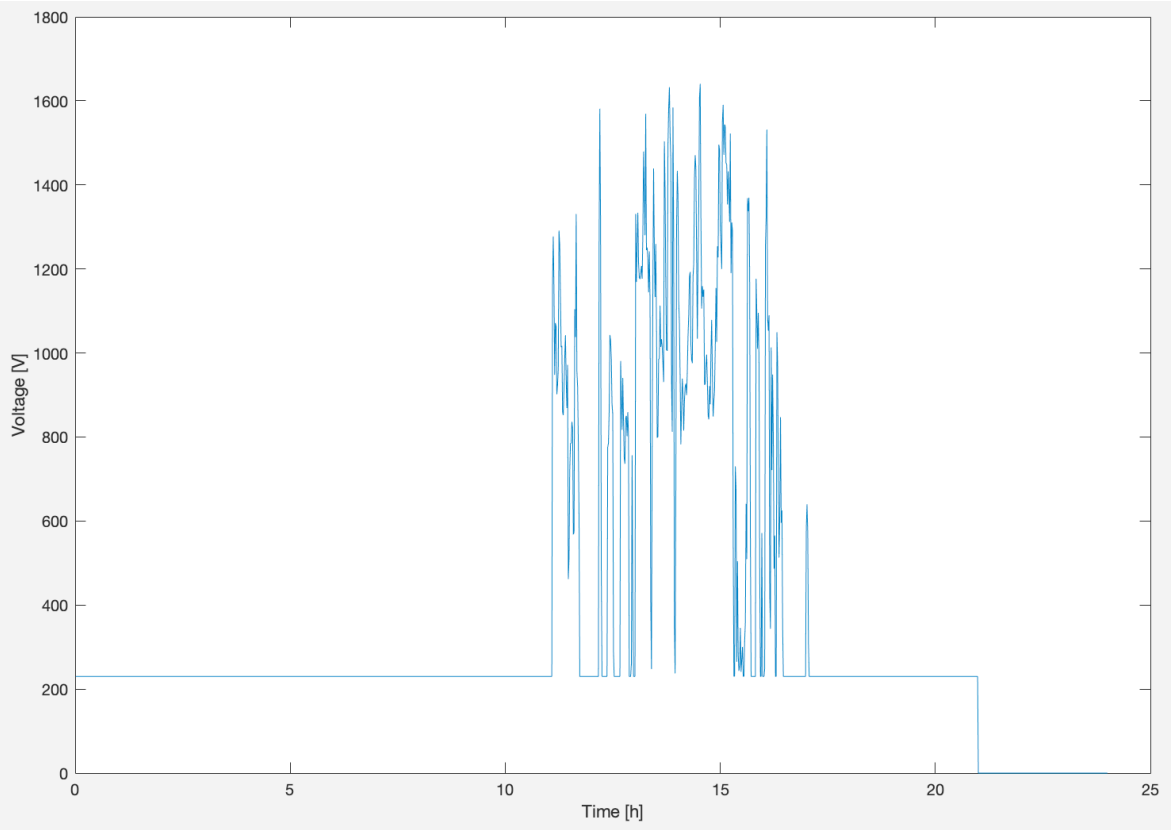

Figure A13.1 Scenario 1: Settlement microgrid system output voltage

Appendix 14 Scenario 2: Settlement battery AC charging / discharging current

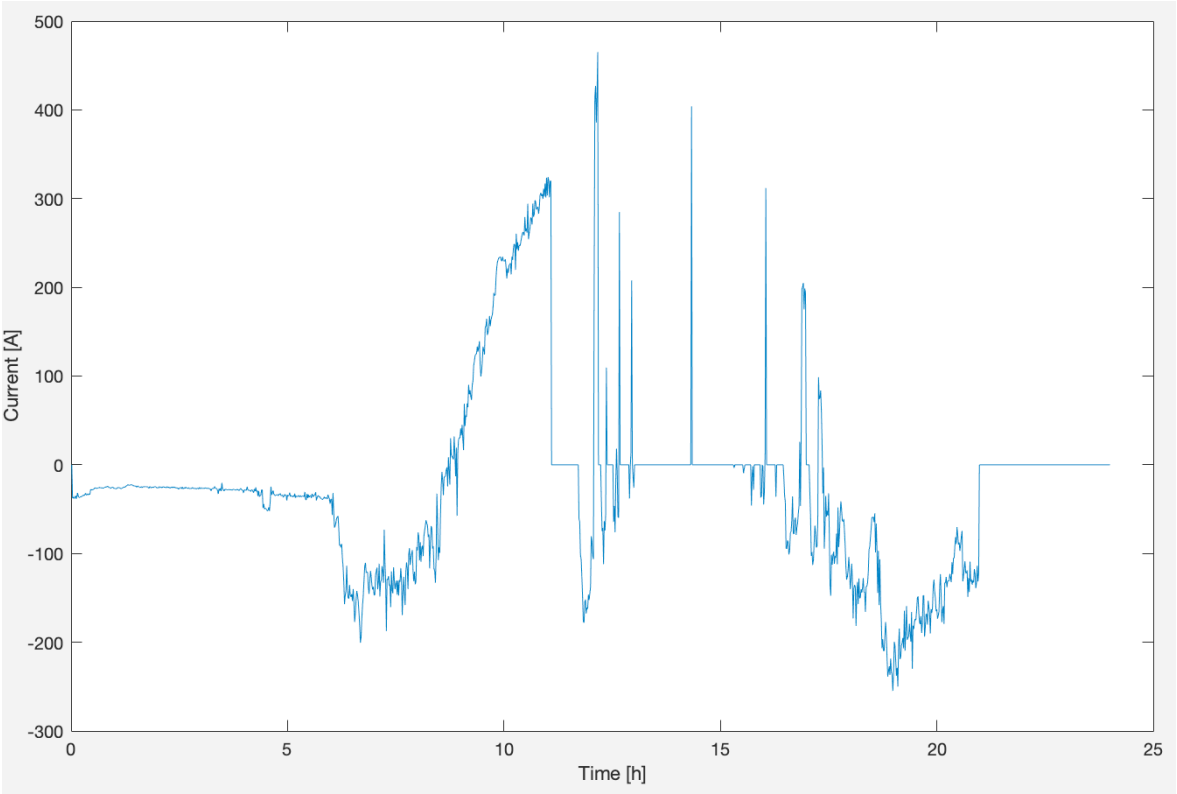

Figure A14.1 Scenario 2: Settlement battery AC charging / discharging current

Appendix 15 Scenario 2: Settlement battery SOC behaviour

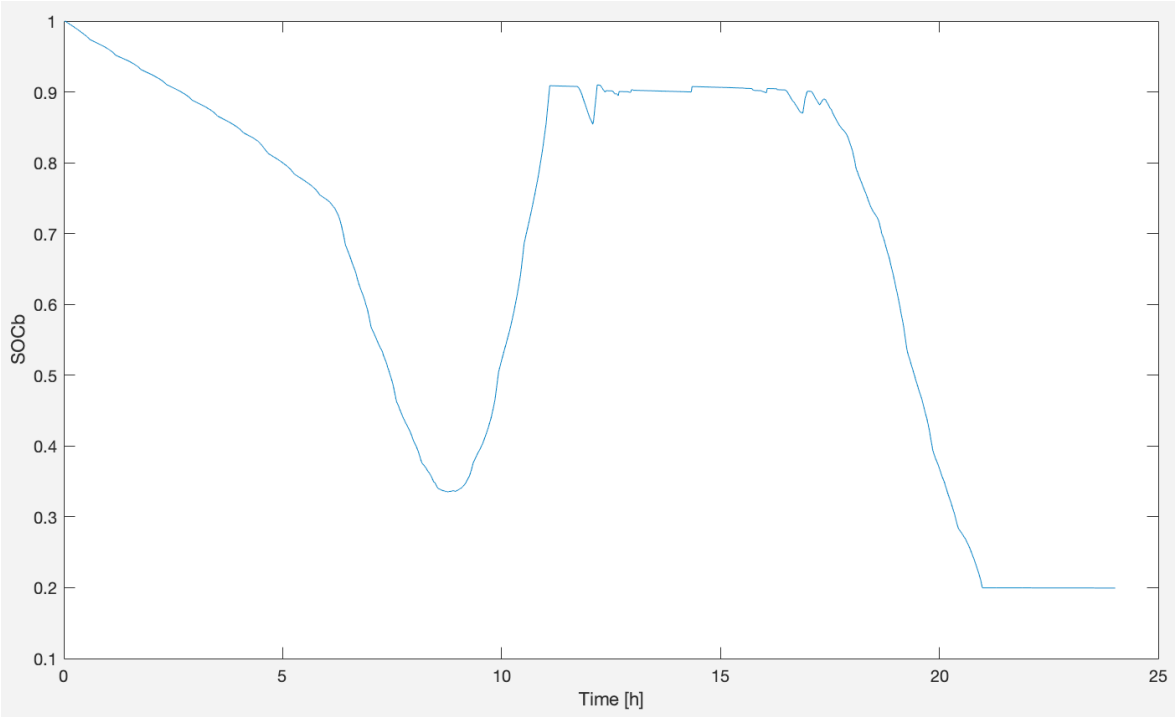

Figure A15.1 Scenario 2: Settlement battery SOC behaviour

Appendix 16 Scenario 2: Settlement flywheel SOC behaviour

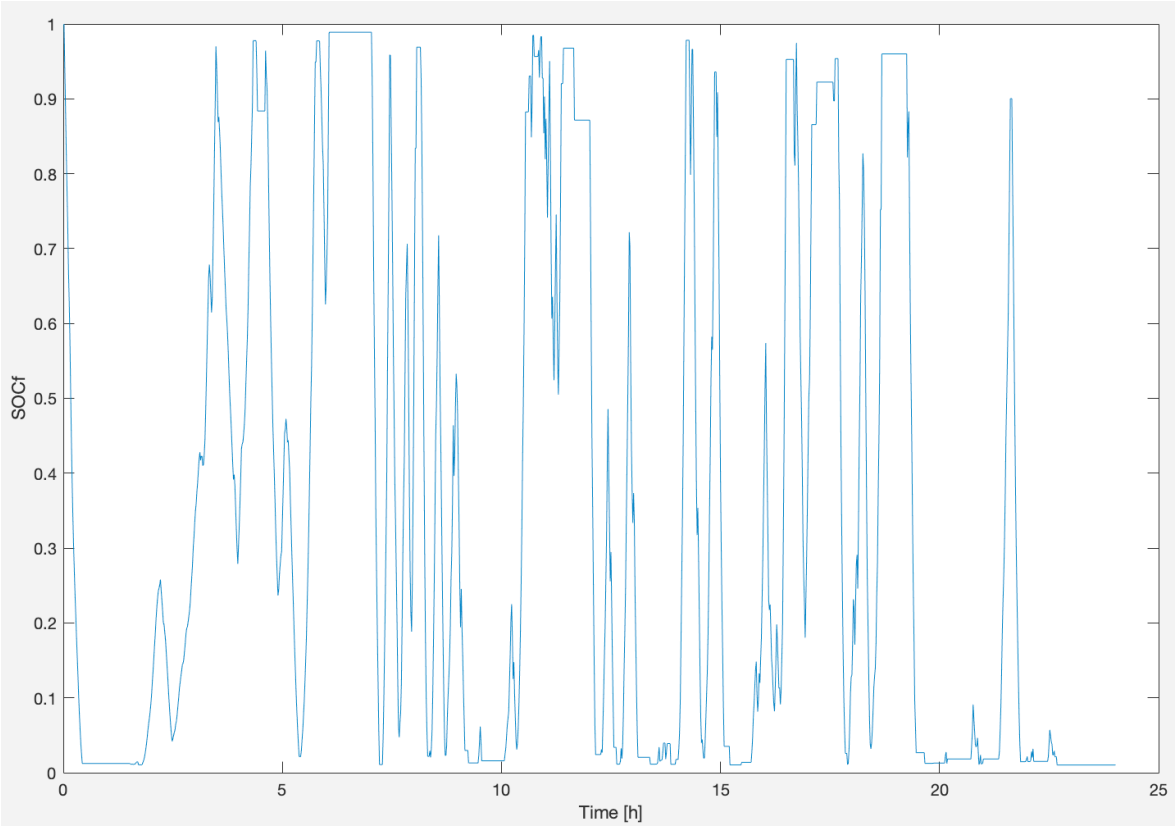

Figure A16.1 Scenario 2: Settlement flywheel SOC behaviour

Appendix 17 Scenario 2: Settlement microgrid system output voltage

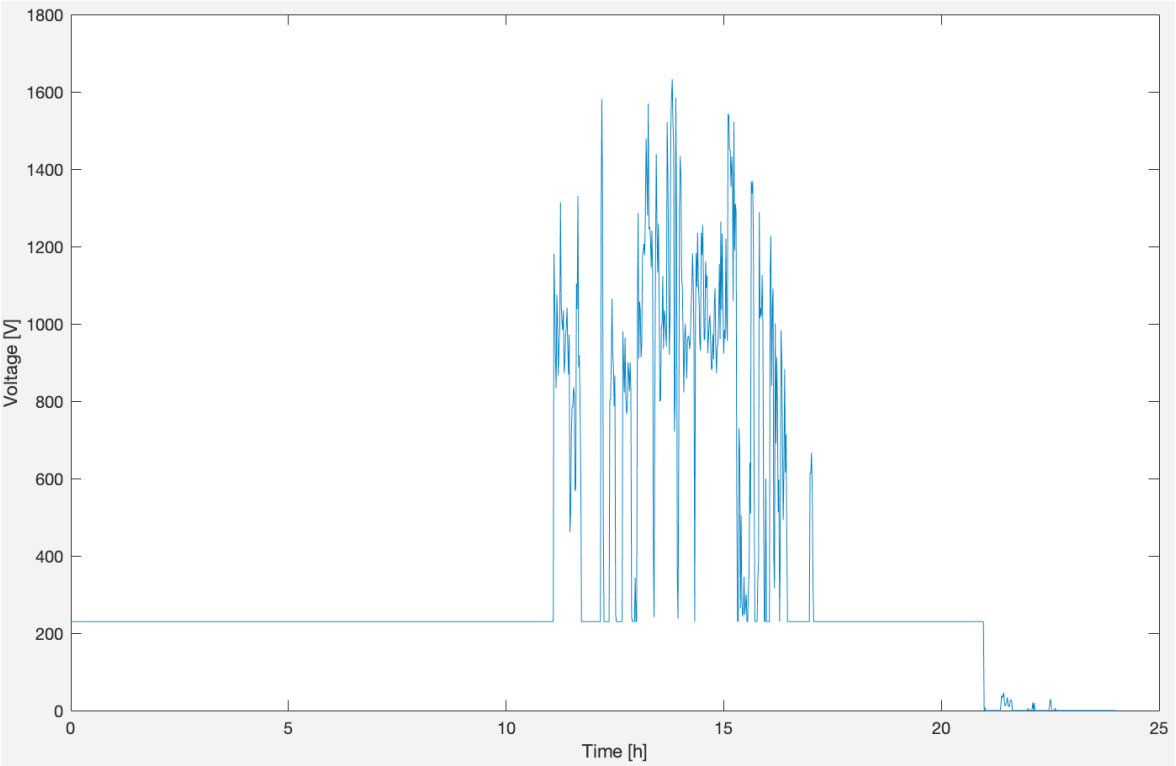

Figure A17.1 Scenario 2: Settlement microgrid system output voltage

Settlement		
	PV and battery storage self-financing	**PV , battery and flywheel self-financing**
Battery storage	20.000 €	20.000 €
Flywheel storage	0 €	660.000 €
Price of PV Moduls	198.633 €	198.633 €
Inverter costs	9.932 €	9.932 €
Small parts	3.000 €	3.000 €
Costs for installation and commissioning of the system	5.000 €	5.000 €
sum of acquisition costs	**236.565 €**	**896.565 €**
lending rates	0 €	0 €
sum of expenses	**236.565 €**	**896.565 €**
Subsidy per year DE	11.417,67 €	11.417,67 €
Saving DE	24.406,46 €	24.406,46 €
Subsidy per year EE	8.911,76 €	8.911,76 €
Saving EE	9.762,58 €	9.762,58 €
running costs	2.366 €	8.966 €
sum of annual income DE	33.458 €	26.858 €
sum of annual income EE	16.309 €	9.709 €
payback period DE [years]	**7**	**33**
payback period EE [years]	**15**	**92**

Figure A18.1 Financial analysis of settlement microgrid